



**HAL**  
open science

## Non-autonomous stomatal control by pavement cell turgor via the $K^+$ channel subunit AtKC1

Manuel Nieves-Cordones, Farrukh Azeem, Yuchen Long, Martin Boeglin, Geoffrey Duby, Karine Mouline, Eric Hosy, Alain Vavasseur, Isabelle Chérel, Thierry Simonneau, et al.

### ► To cite this version:

Manuel Nieves-Cordones, Farrukh Azeem, Yuchen Long, Martin Boeglin, Geoffrey Duby, et al.. Non-autonomous stomatal control by pavement cell turgor via the  $K^+$  channel subunit AtKC1. *The Plant cell*, 2022, 34 (5), pp.2019-2037. 10.1093/plcell/koac038 . hal-03579607

**HAL Id: hal-03579607**

**<https://hal.inrae.fr/hal-03579607>**

Submitted on 18 Feb 2022

**HAL** is a multi-disciplinary open access archive for the deposit and dissemination of scientific research documents, whether they are published or not. The documents may come from teaching and research institutions in France or abroad, or from public or private research centers.

L'archive ouverte pluridisciplinaire **HAL**, est destinée au dépôt et à la diffusion de documents scientifiques de niveau recherche, publiés ou non, émanant des établissements d'enseignement et de recherche français ou étrangers, des laboratoires publics ou privés.



Distributed under a Creative Commons Attribution 4.0 International License

2  
3 **Non-autonomous stomatal control by pavement cell turgor via the K<sup>+</sup> channel**  
4 **subunit AtKC1**5  
6 **Manuel Nieves-Cordones<sup>a,1,g</sup>, Farrukh Azeem<sup>a,3</sup>, Yuchen Long<sup>b,2</sup>, Martin Boeglin<sup>a</sup>, Geoffrey**  
7 **Duby<sup>a</sup>, Karine Mouline<sup>a</sup>, Eric Hosy<sup>a,4</sup>, Alain Vavasseur<sup>c</sup>, Isabelle Chérel<sup>a</sup>, Thierry**  
8 **Simonneau<sup>d</sup>, Frédéric Gaymard<sup>a</sup>, Jeffrey Leung<sup>e</sup>, Isabelle Gaillard<sup>a</sup>, Jean-Baptiste**  
9 **Thibaud<sup>a,f</sup>, Anne-Aliénor Véry<sup>a,g</sup>, Arezki Boudaoud<sup>b,5</sup> and Hervé Sentenac<sup>a,g</sup>**10  
11 <sup>a</sup>Biochimie et Physiologie Moléculaire des Plantes, UMR BPMP, Univ Montpellier, CNRS, INRAE, Montpellier SupAgro, Montpellier 34060, France12 <sup>b</sup>Laboratoire Reproduction et Développement des Plantes, Univ Lyon, ENS de Lyon, UCB Lyon 1, CNRS, INRA, F-69342, Lyon, France13 <sup>c</sup>CEA Cadarache DSV DEVM LEMS UMR 163, CNRS/CEA, F-13108, St Paul Lez Durance, France14 <sup>d</sup>INRA Laboratoire d'Ecophysiologie des Plantes sous Stress Environnementaux, Place Viala, 2, F-34060 Montpellier Cedex 1, France15 <sup>e</sup>Université Paris-Saclay, INRAE, AgroParisTech, CNRS, Institut Jean-Pierre Bourgin (JJPB), 78000, Versailles, France16 <sup>f</sup>Institut des biomolécules Max Mousseron (UMR 5247 CNRS-UM-ENSCM) Campus CNRS, 1919 route de Mende, F-34293 Montpellier Cedex 05,  
17 France18 <sup>1</sup>Present address: Departamento de Nutrición Vegetal, CEBAS-CSIC, Campus de Espinardo, 30100 Murcia, Spain19 <sup>2</sup>Present address: Department of Biological Sciences, National University of Singapore, Singapore 11755820 <sup>3</sup>Present address: Department of Bioinformatics and Biotechnology, Govt. College University, Faisalabad, Pakistan21 <sup>4</sup>Present address: Interdisciplinary Institute for Neuroscience, University of Bordeaux, F-33077 Bordeaux Cedex, France22 <sup>5</sup>Present address: LadHyX, CNRS, Ecole polytechnique, Institut Polytechnique de Paris, 91120, Palaiseau, France23 <sup>g</sup>Corresponding authors: [herve.sentenac@inrae.fr](mailto:herve.sentenac@inrae.fr); [mncordones@cebas.csic.es](mailto:mncordones@cebas.csic.es); [anne-alienor.very@cnrs.fr](mailto:anne-alienor.very@cnrs.fr)24  
25 **Short Title: Stomatal Control by Pavement Cell Turgor**26  
27 **One sentence summary:** Inactivation of the Arabidopsis K<sup>+</sup> channel gene *AtKC1* reveals that interactions  
28 and K<sup>+</sup> shuttling between guard cells, pavement cells and trichomes contribute to the non-autonomous  
29 stomatal responses.30  
31 The author(s) responsible for distribution of materials integral to the findings presented in this article in  
32 accordance with the policy described in the Instructions for Authors  
33 (<https://academic.oup.com/plcell/pages/General-Instructions>) are: Manuel Nieves-Cordones  
34 ([mncordones@cebas.csic.es](mailto:mncordones@cebas.csic.es)) and Anne-Aliénor Véry ([anne-alienor.very@cnrs.fr](mailto:anne-alienor.very@cnrs.fr))35  
36 **Abstract**37  
38 Stomata optimize land plants' photosynthetic requirements and limit water vapor loss. So far, all of the  
39 molecular and electrical components identified as regulating stomatal aperture are produced and operate  
40 directly within the guard cells. However, a completely autonomous function of guard cells is inconsistent  
41 with anatomical and biophysical observations hinting at mechanical contributions of epidermal origins.  
42 Here, K<sup>+</sup> assays, membrane potential measurements, microindentation and plasmolysis experiments  
43 provide evidence that disruption of the *Arabidopsis thaliana* K<sup>+</sup> channel subunit gene *AtKC1* reduces  
44 pavement cell turgor, due to decreased K<sup>+</sup> accumulation, without affecting guard cell turgor. This results in  
45 an impaired back-pressure of pavement cells onto guard cells, leading to larger stomatal apertures. Poorly  
46 rectifying membrane conductances to K<sup>+</sup> were consistently observed in pavement cells. This plasmalemma  
47 property is likely to play an essential role in K<sup>+</sup> shuttling within the epidermis. Functional complementation  
48 reveals that restoration of the wild-type stomatal functioning requires the expression of the transgenic  
49 *AtKC1* at least in the pavement cells and trichomes. Altogether, the data suggest that *AtKC1* activity  
50 contributes to the building of the back-pressure that pavement cells exert onto guard cells by tuning K<sup>+</sup>  
51 distribution throughout the leaf epidermis.

54

55

56

57 **INTRODUCTION**

58

59 In land plants, the epidermis is covered by a non-permeable waxy cuticle and diffusion of CO<sub>2</sub>  
60 from the atmosphere to inner photosynthetic tissues takes place through microscopic pores  
61 present on the leaf surface. Each of these pores is surrounded by a pair of osmocontractile cells,  
62 named guard cells, together forming a stoma. The physical continuum provided by the stomata  
63 between the leaf inner tissue and the atmosphere also enables transpiration, which has however  
64 to be tightly controlled to avoid desiccation.

65 The epidermis comprises three main types of clonally related cells: pavement cells, guard  
66 cells, and trichomes. Embedded within the epidermal cell layer, guard cells can be in direct contact  
67 with surrounding pavement cells (e.g., in *Arabidopsis thaliana*; Supplemental Figure S1, left photo  
68 column), or associated with subsidiary cells (Nguyen et al., 2017) to form a stomatal complex  
69 (Gray et al., 2020). The molecular and osmotic machinery responsible for the changes in guard  
70 cell turgor that either open (Tominaga et al., 2001; Jammes et al., 2014) or close the stomatal pore  
71 has been deeply investigated (Jezek and Blatt, 2017). All components regulating stomatal  
72 movements, even the cell-to-cell mobile abscisic acid (ABA) stress hormone (Bauer et al., 2013),  
73 are produced and act directly within the guard cells. For instance, in response to low atmospheric  
74 or soil humidity, ABA initiates stomatal closing by binding to a subfamily of cytosolic receptors  
75 within the guard cells to activate a phosphorylation-based signaling cascade leading to reduced  
76 cell turgor by modulating interdependent H<sup>+</sup>, K<sup>+</sup> and anion fluxes (Hedrich, 2012; Jezek and Blatt,  
77 2017). In angiosperms, mature guard cells are thought to lack plasmodesmata with adjoining cells  
78 (Wille and Lucas, 1984; Palevitz and Hepler, 1985), reinforcing the notion of their self-sufficient  
79 functioning. Highly-purified guard cell protoplasts have been extensively used to characterize in  
80 detail the ABA-induced events that include changes in ion transport activities (Jezek and Blatt,  
81 2017) as well as transcriptomic (Leonhardt et al., 2004; Wang et al., 2011), proteomic (Zhao et al.,  
82 2008) and metabolomic profiles (Jin et al., 2013; Misra et al., 2015; Zhu and Assmann, 2017).

83 Potassium (K<sup>+</sup>) is a major osmoticum in this machinery (Humble and Raschke, 1971; Talbott  
84 and Zeiger, 1996; Hedrich, 2012; Jezek and Blatt, 2017; Britto et al., 2021). K<sup>+</sup> fluxes into, or out  
85 of, guard cells, resulting in stomatal opening or closure, respectively, involve voltage-gated K<sup>+</sup>  
86 channels of the Shaker family (Blatt, 2000; Véry and Sentenac, 2003; Pandey et al., 2007; Kim et  
87 al., 2010; Hedrich, 2012; Véry et al., 2014). Gene expression studies, electrophysiological  
88 analyses and reverse genetics approaches carried out in *Arabidopsis* have revealed that K<sup>+</sup> influx

89 into guard cells, leading to stomatal opening, is strongly dependent on expression of the inwardly  
90 rectifying hyperpolarization-activated Shaker K<sup>+</sup> channels KAT1 and KAT2 (K<sup>+</sup> channel in  
91 *Arabidopsis thaliana* 1 and 2) (Lebaudy et al., 2008 and 2010), while the efflux of K<sup>+</sup> from guard  
92 cells, allowing stomatal closure, involves expression of the outwardly rectifying depolarization-  
93 activated Shaker K<sup>+</sup> channel GORK (Hosy et al., 2003).

94 The large body of cellular and molecular information leads to the conclusion that guard cells  
95 possess all necessary molecular and electrical components in stomatal control. This  
96 understanding is, however, unmoored from the biophysical and anatomical approaches of  
97 stomatal regulation within its epidermal context, in which the embedded guard cells are subjected  
98 to mechanical and physiological exertions from their neighboring pavement/subsidiary cells (Jezek  
99 et al., 2019). For example, stomatal conductances can show considerable micro-heterogeneity in  
100 the leaf even when this organ is kept in a constant environment. This has been attributed to  
101 variable or unstable hydraulic interactions between guard cells with their surrounding pavement  
102 cells, usually within leaf sectors defined anatomically by vein patterns (Mott and Buckley, 2000).  
103 Also, at the cell level, when a series of reductions of turgor are experimentally imposed on both  
104 guard and pavement cells of epidermal strips, by increasing the concentration of an osmotically  
105 active solute in the external solution, the stomatal aperture does not narrow, as would be expected  
106 if guard cells responded independently of pavement cells. Rather, the pore aperture will widen in a  
107 first phase. When the concentration of the external solute is further increased, the stomatal  
108 aperture will then narrow in a more gradual second phase. In contrast, if the turgor of the  
109 pavement/subsidiary cell is selectively ablated, the stomatal aperture will simply narrow in a  
110 “monotonic” way with the increase in external solute concentration (MacRobbie, 1980). These  
111 observations suggest that, within an epidermal layer, the stomatal aperture is not autonomously  
112 regulated, but conjointly set by, at least, the relative turgor that opposes the guard cells with the  
113 surrounding pavement cells. Much is still unknown about the mechanisms that underlie the non-  
114 autonomous stomatal response, such as the molecular, cellular and physiological bases of the  
115 interacting mechanisms, and the responsible epidermal cell types or their locations in the leaf.  
116 Here we show that the Shaker channel gene *AtKC1* (*Arabidopsis thaliana* K<sup>+</sup> channel 1)  
117 (accession number AT4G32650) contributes to these mechanisms.

118 Shaker channels, which dominate the plasma membrane conductance to K<sup>+</sup> in most cell  
119 types, are encoded by a family of nine members in *Arabidopsis* (Véry et al., 2014). These  
120 channels are sensitive to voltage and activated by either membrane depolarization for K<sup>+</sup> efflux  
121 (outwardly rectifying channels), or membrane hyperpolarization allowing K<sup>+</sup> influx (inwardly  
122 rectifying channels). They are tetrameric proteins, and the four subunits that assemble to form a  
123 functional protein can be encoded by the same Shaker gene (giving rise to a homotetrameric

channel) or by different Shaker genes (heterotetrameric channel) (Daram et al., 1997; Urbach et al., 2000; Jegla et al., 2018). The Shaker subunit encoded by *AtKC1* (At4G32650) has been termed a "silent" Shaker channel subunit (Reintanz et al., 2002) because it does not form functional channels on its own but only when in complex with other inwardly rectifying channel subunits to modulate the functional properties of the channel, including voltage sensitivity (Duby et al., 2008; Geiger et al., 2009; Honsbein et al., 2009; Jeanguenin et al., 2011; Zhang et al., 2015; Wang et al., 2016).

*AtKC1* is expressed in roots and in leaves (Reintanz et al., 2002; Pilot et al., 2003). In the root, it is expressed in the periphery cells, where it associates with the AKT1 inward Shaker subunit and thereby plays a role in channel-dependent K<sup>+</sup> uptake from the soil (Geiger et al. 2009; Honsbein et al. 2009). In leaves, *AtKC1* is expressed in the whole epidermal tissue, i.e., in trichomes, hydathodes, pavement cells and guard cells (Pilot et al., 2003; Figure S1), in contrast to the two other well-studied inward Shaker channel genes *KAT1* and *KAT2* whose expression pattern in the leaf epidermis is restricted to guard cells (Nakamura et al., 1995; Pilot et al., 2001). In this report, we show that *AtKC1* contributes to stomatal aperture regulation by modulating conflicting turgors of guard cells and surrounding pavement cells.

## RESULTS

### Disruption of *AtKC1* Impairs the Control of Stomatal Aperture

The role of *AtKC1* in the leaf epidermis was investigated using a loss-of-function *Arabidopsis* line, *atkc1-2*, obtained in the Wassilewskija (Ws) ecotype (Jeanguenin et al., 2011). Leaves excised from *atkc1-2* plants were found to lose more water than leaves excised from wild-type (WT) plants (Figure 1A). Furthermore, stomatal conductance measured in intact leaves (Figure 1B) and transpiration rates in whole-plant assays during both light and dark periods (Figure 1C) were larger in *atkc1-2* than in WT plants. In agreement with these observations, *in vitro* measurements of stomatal aperture on leaf epidermal strips yielded larger values in *atkc1-2* than in WT plants, regardless of dark or light conditions (stimuli of stomatal closure and opening, respectively) (Figure 1D). Stomatal density was not affected by the *atkc1-2* mutation (Figure S2). Transformation of the *atkc1-2* mutant with a construct allowing expression of *AtKC1* under the control of its own promoter region led to a wild-type phenotype in each of these experiments (Figures 1A-D), providing evidence that the stomatal defects of the *atkc1-2* mutant plants resulted from the absence of *AtKC1* functional expression.

## 159 Patch-clamp analyses of the membrane conductance to K<sup>+</sup> in epidermal cells

160  
161 The patch-clamp technique was used to investigate the membrane conductance to K<sup>+</sup> in  
162 protoplasts enzymatically obtained from wild-type and *atkc1-2* epidermal strips. The  
163 electrophysiological recordings carried out in wild-type guard cell protoplasts yielded a classical  
164 current-voltage curve, displaying the typical strong rectification of both the inward and outward K<sup>+</sup>  
165 currents (Figure 2) in agreement with literature data (Schroeder et al., 1987; Hosy et al., 2003;  
166 Lebaudy et al., 2008). This rectification results from the fact that the K<sup>+</sup> channels mediating K<sup>+</sup>  
167 transport across the guard cell membrane are either activated by membrane hyperpolarization and  
168 dedicated to K<sup>+</sup> influx, or activated by membrane depolarization and then dedicated to K<sup>+</sup> efflux.  
169 Within a large range of voltages, from ca. -150 to 0 mV in the experiment described by Figure 2,  
170 the two populations of channels are inactive and the membrane is almost impermeable to K<sup>+</sup>.  
171 Such channels are said to be "rectifiers": they mediate a K<sup>+</sup> current in only one direction, either  
172 into or out from the cell. Very similar current-voltage curves were obtained in the WT and in the  
173 *atkc1-2* mutant (Figure 2), which led to the conclusion that the absence of *AtKC1* expression had  
174 no significant impact on the membrane conductance to K<sup>+</sup> in guard cells.

175 No patch-clamp analysis of pavement cell protoplasts has been reported in Arabidopsis to  
176 our knowledge. Protoplasts from pavement cells were obtained by shorter enzymatic cell-wall  
177 digestion compared to guard cell protoplasts. Pavement cell protoplasts could be distinguished  
178 from guard cell protoplasts based on their larger size, and from contaminating mesophyll  
179 protoplasts (if any in the preparation) based on the absence of chloroplasts.

180 Different types of current traces could be distinguished in the WT pavement cell protoplasts  
181 (Figure 3 and Figure S3A-C). The recorded traces/protoplasts were operationally sorted into two  
182 major categories, according to the presence (Figure 3) or absence (see below, Figure S3A-C) of  
183 an inward current component displaying a time-dependent activation, reminiscent of a Shaker-type  
184 slowly activating conductance (Véry and Sentenac, 2002).

185 The membrane conductance to K<sup>+</sup> of WT protoplasts displaying the Shaker-type slowly  
186 activating currents was analyzed in more detail. The current-voltage (I-V) curve obtained for this  
187 type of protoplast in the presence of 105 mM K<sup>+</sup> in the external solution (Figure 3B and E, black  
188 symbols) crosses the x axis close to the K<sup>+</sup> equilibrium potential, estimated to be close to -7 mV  
189 (the K<sup>+</sup> concentration of the pipette solution and external bath being close to 140 and 105 mM,  
190 respectively), as expected since K<sup>+</sup> was the single permeable ion present at a high concentration  
191 in these solutions. A major result is that these I-V curves reveal a rather low level of rectification  
192 (Figure 3B and E), when compared with that displayed by the guard cell I-V curve (Figure 2).  
193 Adding 10 mM Ba<sup>2+</sup> (a classical K<sup>+</sup> channel blocker: Schroeder et al., 1987; Wegner et al., 1994;

194 Roelfsema and Prins, 1997; Pilot et al., 2001; Su et al., 2005; Rohaim et al., 2020) resulted in a  
195 strong inhibition of the recorded currents (Figure 3A-C), the magnitude of the inhibition appearing  
196 to be slightly voltage-dependent (Figure 3C). Decreasing the external concentration of  $K^+$  from 105  
197 mM to 15 mM shifted the current reversal potential by about  $-40$  mV (Figure 3D-E; theoretical shift  
198 by ca.  $-49$  mV expected for a membrane permeable to  $K^+$  only). Altogether, these results indicated  
199 that the currents were mainly channel mediated and carried by  $K^+$  ions.

200 Patch-clamp recordings were carried out in parallel experiments (alternating measurements  
201 on WT and mutant plants grown simultaneously) to compare the electrical properties of pavement  
202 cell protoplasts from WT and *atkc1-2* plants. Among 28 protoplasts from WT pavement cells, 10  
203 (ca. 36%) belonged to the first category, i.e., displaying a Shaker-type time-dependent activation  
204 of inward currents (as shown in Figure 3F). In agreement with the data shown by Figure 3B and E,  
205 the I-V curve obtained from these 10 protoplasts displays a low level of rectification (Figure 3H,  
206 black symbols). In the second category of protoplasts, i.e. characterized by the absence of an  
207 inward current component displaying a time-dependent activation (18 protoplasts out of the 28  
208 ones), at least three patterns of current traces could be identified (Figure S3A-C). The current-  
209 voltage curves corresponding to these recordings also displayed a rather weak level of rectification  
210 (lower panels in Figure S3A-C), when compared with that observed in guard cell protoplasts  
211 (Figure 2). The current recordings obtained in the *atkc1-2* mutant protoplasts could be sorted into  
212 the same categories as those defined for the WT protoplasts, according to the presence or  
213 absence of a detectable time-dependent inward Shaker-type component. From 32 protoplasts, 8  
214 (25%) displayed such a component (Figure 3G), which was also characterized by a low level of  
215 rectification (Figure 3H, open symbols), and 24 protoplasts belonged to the other category (Figure  
216 S3D-F). No significant impairment of the membrane conductance to  $K^+$  was detected in the  
217 *atkc1-2* protoplasts classified as belonging to the former category, i.e., displaying the Shaker-type  
218 component, when compared with the corresponding WT protoplasts (Figure 3H). In the other  
219 category, each of the different types of current patterns that were recorded in the *atkc1-2*  
220 pavement cell protoplasts seemed to have a counterpart amongst the current patterns observed in  
221 the corresponding WT protoplasts (Figure S3). This whole set of data did not provide evidence  
222 that the *atkc1-2* mutation affected the membrane conductance to  $K^+$  in every pavement cell.

## 223 224 **Loss of *AtKC1* Expression in Guard Cells Does Not Underlie the *atkc1-2* Mutant Stomatal** 225 **Phenotype**

226  
227 *AtKC1* transcripts were found to be at higher levels, by about 5 times, in whole leaf extracts than in  
228 guard cells (Figure 4, A right panel). Furthermore, *AtKC1* transcripts in guard cell protoplasts were

at lower levels than those of *KAT1* and *KAT2* (Figure 4A, left panel), the major contributors to the Shaker inward conductance in guard cells (Lebaudy et al., 2008 and 2010; Hedrich, 2012).

In the epidermis, the *KAT1* promoter (*ProKAT1*) is specifically active in guard cells (Nakamura et al., 1995). A *ProKAT1:AtKC1* construct introduced into *atkc1-2* mutant plants did not rescue the stomatal phenotype of *atkc1-2* in the dark, in the light and after a treatment with the stress hormone ABA, well known to induce stomatal closure (Figure 4B). Detection of *AtKC1* transcripts in leaves of *atkc1-2* mutant plants transformed with this *ProKAT1:AtKC1* construct (Figure S4A) provided first evidence that the absence of complementation was not due to expression issues. A crucial objective was then to check whether the *ProKAT1* promoter was actually active and allowed expression of *AtKC1* subunits in guard cells of the *atkc1-2* mutant in the experimental conditions that had previously allowed the defect in stomatal aperture control to be observed in the *atkc1-2* mutant (Figure 1). *In planta*, we did not succeed in detecting the fluorescence of *AtKC1*-GFP translational fusions expressed under the control of the *ProKAT1* promoter (or under control of any of the promoters described below when stably expressed in *Arabidopsis* transgenic plants). So far, to our knowledge, translational *AtKC1*-GFP fluorescence in plant cells has only been observed with strong constitutive promoters such as that from the gene of an H<sup>+</sup>-ATPase (Duby et al., 2008; Jeanguenin et al., 2011; Nieves-Cordones et al., 2014) or 35S (Honsbein et al., 2009). We thus developed an alternative strategy by taking advantage of the fact that *AtKC1* can associate with the guard cell *KAT1* and *KAT2* inward Shaker channel subunits and thereby form heteromeric channels (Jeanguenin et al., 2011) to develop a dominant negative approach as described by Lebaudy et al. (2008). A dominant-negative form of *AtKC1*, *AtKC1-DN*, was substituted for *AtKC1* in the previous *ProKAT1:AtKC1* construct. *AtKC1-DN* encodes a mutated channel subunit (obtained by site-directed mutagenesis) in which large and positive residues (R) are present in the pore region (Jeanguenin et al., 2011). These residues plug the channel permeation pathway when *AtKC1-DN* subunits associate with other inwardly rectifying Shaker subunits, including *KAT1* and *KAT2* (Jeanguenin et al., 2011). After introduction into the *atkc1-2* mutant, the new construct, *ProKAT1:AtKC1-DN*, was found to reduce stomatal aperture (Figure S4B), providing evidence that *AtKC1-DN* was expressed in *atkc1-2* mutant guard cells, inhibiting inward channel activity, and thus that *ProKAT1* was actually active in *atkc1-2* guard cells under our experimental conditions. Altogether, these results provided the first indication that the absence of *AtKC1* expression in guard cells alone could not be considered as the main cause of the *atkc1-2* mutant stomatal phenotype.

## Disruption of *AtKC1* Results in Decreased K<sup>+</sup> Accumulation in Leaf Epidermis and Reduced Turgor Pressure in Pavement Cells



265 K<sup>+</sup> contents were measured in whole leaves, in leaf margins (isolated 2-mm-width strips) enriched  
266 with hydathodes and in epidermal strips. Compared to the WT, the overall K<sup>+</sup> status of *atkc1-2* was  
267 not substantially altered in whole leaves (Figure 5), in agreement with previous analyses  
268 (Jeanguenin et al., 2011), nor was it altered in leaf margins (Figure 5). In contrast, K<sup>+</sup> contents in  
269 epidermal strips were significantly lower, by 42 mM, in the mutant than in wild-type plants, when  
270 compared on a fresh weight basis (from Figure 5, the FW/DW ratio being  $9.3 \pm 0.3$ ,  $n = 12$ ). Such  
271 a difference in K<sup>+</sup> content between *atkc1-2* and WT plants could hardly be ascribed to guard cells  
272 alone but rather to pavement cells, because of the relatively lower abundance and volume of  
273 guard cells in the leaf epidermis (see Figure S1).

274 The hypothesis that reduced K<sup>+</sup> contents in *atkc1-2* pavement cells would decrease the  
275 turgor of these cells was then checked via three independent experimental approaches. First,  
276 recent improvements in atomic force microscopy (AFM) allowed us to quantify turgor pressure in  
277 living plant cells (Beauzamy et al., 2015). Data obtained under similar conditions as those used for  
278 *in vitro* measurements of stomatal aperture in epidermal strips (under light and in the presence of  
279 stomatal aperture solution; Figure 1D and 4B) showed that the pavement cell turgor pressure was  
280 weaker (by  $\sim 0.15$  MPa) in *atkc1-2* than in WT plants (Figure 6, A left panel). In contrast,  
281 measurements performed in parallel on the same leaves in the same experimental conditions did  
282 not reveal any significant difference in guard cell turgor between the WT and *atkc1-2* plants  
283 (Figure 6A, right panel), providing further support to the hypothesis that AtKC1 plays a role in  
284 regulating stomatal aperture from another cell type than guard cells. During these measurements,  
285 we have also noted that within the same wild-type leaf, the turgor pressure was higher, on average  
286 by about 2 times, in the guard cells than in the pavement cells (Figure 6A; note the difference in y  
287 axis scale between the left and right panels).

288 In a second series of experiments, we assessed the effects of increasing the concentration of  
289 mannitol in the solution bathing epidermal strips on pavement cell plasmolysis. Relative to the WT,  
290 40 to 60 mM less mannitol was needed to plasmolyze 50% of *atkc1-2* pavement cells (Figure 6B),  
291 which indicated reduced osmotically active solute contents in *atkc1-2* pavement cells.

292 The third series of experiments was inspired by classical analyses of the effects of external  
293 medium osmolarity on stomatal aperture. MacRobbie (1980) showed that stomatal aperture in  
294 epidermal strips responded differently to increasing the external osmolarity depending on whether  
295 the surrounding pavement cells were dead (killed by acid treatment) or alive (see Introduction).  
296 We investigated the relationship between stomatal aperture and external medium osmolarity, this  
297 time independently of the alive/dead status of the pavement cells, but rather in the presence or  
298 absence of *AtKC1* expression. Stomatal aperture was measured in epidermal strips bathed in

standard medium (as in Figure 1D experiment) supplemented with mannitol at increasing concentrations in order to raise the external osmolarity. In *atkc1-2* epidermal strips, the stomatal aperture decreased monotonically (Figure 6C). Conversely, in WT epidermal strips, the stomatal aperture displayed a slight increase in a first step, and then decreased when the mannitol concentration was further increased (Figure 6C). Such a non-monotonic relationship between extracellular osmotic potential and stomatal aperture is reminiscent of the results of MacRobbie (1980) discussed above. It can be classically explained as follows. Increasing the external osmolarity decreases the turgor of both the guard cells and the pavement cells by the same amount. The resulting turgor reduction in pavement cells tends to increase the stomatal aperture, while in guard cells it tends to reduce this aperture. The balance of these opposite effects determines the final stomatal aperture at a given external osmolarity. Thus, the relation between stomatal aperture and the external osmolarity can be non-monotonic. Reciprocally, such a non-monotonic response provides evidence that guard cell turgor is not the only determinant of stomatal aperture and that the turgor of the surrounding pavement cells exerts a back-pressure onto guard cells, thereby playing a role in the control of stomatal aperture. The results displayed in Figure 6C therefore indicate that a back-pressure was exerted on guard cells by surrounding pavement cells in WT epidermal strips, but that this phenomenon did not occur in *atkc1-2* epidermal strips.

Altogether, these 3 series of experiments indicated that reduced  $K^+$  contents decreased the turgor in *atkc1-2* pavement cells and thereby the back-pressure that these cells can exert onto guard cells. They thus provided evidence that AtKC1 contributes to control of stomatal aperture from the surrounding pavement cells.

### Membrane potential measurements in pavement cells

Electrical consequences of the *atkc1-2* mutation in pavement cells were looked for *in planta* by recording the resting membrane potentials (MP) successively at two different external  $K^+$  concentrations, 0.1 mM and 10 mM, using the microelectrode impalement technique. Significantly less negative MP values were recorded in *atkc1-2* mutant plants, when compared with WT control plants, by ca. 20 mV and 48 mV at 0.1 mM and 10 mM  $K^+$ , respectively (Figure 7A). The observation of less negative membrane potentials in pavement cells of the mutant plants is consistent with the lower  $K^+$  content of the epidermis displayed by these plants, when compared to the WT control plants (Figure 5 and 6B). In such experiments, the magnitude of the membrane depolarization induced by an increase in external  $K^+$  is classically interpreted as reflecting the relative  $K^+$  permeability of the membrane (Spalding et al., 1999). The depolarization induced in pavement cells by the increase in  $K^+$  concentration from 0.1 to 10 mM was significantly smaller in

334 the WT than in *atkc1-2* pavement cells (Figure 7B-D), revealing a higher relative K<sup>+</sup> permeability in  
335 the *atkc1-2* mutant cells, which is consistent with the role of AtKC1 as a negative regulator of  
336 Shaker inward K<sup>+</sup> channels (Jeanguenin et al. 2011; see Discussion).

### 338 **Expression of AtKC1 in Several Epidermal Cell Types is Required to Complement the** 339 ***atkc1-2* Mutant Stomatal Phenotype**

340  
341 AtKC1 was expressed in *atkc1-2* mutant plants using different promoters with overlapping  
342 epidermal cell-specificity to determine further cell types, besides pavement cells, in which AtKC1  
343 would affect stomatal aperture control: *ProCER5* (*At1G51500*) (Pighin et al., 2004), *ProOCT3*  
344 (*At1G16390*) (Kufner and Koch, 2008), *ProGL2* (*At1G79840*) (Szymanski et al., 1998), promoter of  
345 the *Uncharacterized Protein Kinase* gene *At1G66460* (Jakoby et al., 2008), *ProFMO1*  
346 (*At1G19250*) (Olszak et al., 2006), *ProCYP96A4* (*At5G52320*) and *ProKCS19* (*At5G04530*). The  
347 expression patterns of these promoters were experimentally confirmed in transgenic Arabidopsis  
348 by fusing them to the *GUS* reporter gene. These observed patterns (Figure S1 and Table 1; see  
349 description below) were entirely consistent with the eFP Browser data (Table S1).

350 Each of these 7 promoters was used to direct transgenic expression of AtKC1 in the *atkc1-2*  
351 mutant tissues. The capacity of the transgenes to complement the mutant phenotype was checked  
352 in a first series of experiments by measuring stomatal aperture in the transformed plants (T3  
353 homozygous transgenic lines) in light conditions as previously performed for the complementing  
354 construct *ProAtKC1:AtKC1* and the non-complementing one *ProKAT1:AtKC1* (Figure 4B).

355 Five of the seven constructs were found not to complement the mutant stomatal phenotype  
356 (Figure 8, panel A, and Table 1). These were *ProKCS19:AtKC1*, *ProOCT3:AtKC1*, *ProGL2:AtKC1*,  
357 *ProAt1G66460:AtKC1* and *ProFMO1:AtKC1* (Figure 8A). The results in Figure S1 indicate that  
358 *ProKCS19* and *ProOCT3* are active in both guard cells and pavement cells, and for the latter, in  
359 hydathodes as well. *ProGL2* and *ProAt1G66460* are active only in trichomes, and *ProFMO1* is  
360 active only in hydathodes (Figure S1).

361 In contrast to the above, two constructs complemented the phenotype as efficiently as  
362 *ProAtKC1:AtKC1* (Figure 4B). These were *ProCER5:AtKC1* and *ProCYP96A4:AtKC1* (Figure 8A).  
363 The GUS staining data displayed in Figure S1 indicate that *ProCER5* (shown to be epidermis-  
364 specific; Pighin et al., 2004) is active in guard cells, pavement cells, hydathodes and trichomes  
365 (abaxial and adaxial sides). *ProCYP96A4* (also leaf epidermis-specific as shown by Mustroph et  
366 al., 2009) is active in guard cells, pavement cells and trichomes (abaxial and adaxial sides) but not  
367 in hydathodes. It should be noted that leaves of Wassilewskija ecotype plants harbor trichomes at

368 both the abaxial and adaxial faces (Telfer et al., 1997) (Figure S5) and that the *atkc1-2* mutation  
369 did not affect trichome density on either face (Figure S6).

370 In a second series of experiments, both the *ProCER5:AtKC1* and *ProCYP96A4:AtKC1*  
371 constructs were found to also restore the stomatal aperture to the wild-type non-monotonic mode  
372 in responding to rising external mannitol concentration – in contrast to *ProKAT1:AtKC1* (Figure 8B  
373 compared with Figure 6C) - and the level of K<sup>+</sup> accumulation in leaf epidermis (Figure 8C  
374 compared with Figure 5).

375 By cross-comparing these data, complementation of the defect in stomatal aperture control of  
376 *atkc1-2* plants required *AtKC1* expression not only in surrounding pavement cells but,  
377 unexpectedly, also in trichomes. However, targeted transgenic expression in only trichomes by  
378 two different specific promoters (*ProGL2* and *ProAt1G66460*) did not rescue the *atkc1-2*  
379 phenotype.

## 381 DISCUSSION

382  
383 Relative to autonomous stomatal control, the non-autonomous regulatory mechanism is  
384 conceptually more abstract, as there had been a paucity of functionally defined genetic or  
385 molecular components. Neither had there been detailed knowledge on the precise cell types from  
386 which these components operated, nor their physiological modes of action. We report here that  
387 the inactivation of *AtKC1* results in larger stomatal apertures and increased transpirational water  
388 loss. *AtKC1* encodes a silent Shaker channel subunit because it does not form functional K<sup>+</sup>  
389 channels on its own (see below). The *atkc1-2* mutation was not compensated by transgenic  
390 expression of *AtKC1* only in guard cells within the leaf epidermis using the promoter of the Shaker  
391 channel gene *KAT1* (Figure 4B). The dominant-negative approach by expressing *ProKAT1:AtKC1-*  
392 *DN* (Figure S4) proved that *ProKAT1* remained active in the guard cells throughout our  
393 experiment. Altogether, these results suggested that *AtKC1* does not control stomatal aperture  
394 from within the guard cells, but that it contributes to the non-autonomous mechanism that opposes  
395 the guard cells' outward push.

396 Turgor pressures of the guard cell and surrounding pavement cells have rarely been directly  
397 measured. Due to their small size, Arabidopsis guard cells are not easily amenable to  
398 investigations using the classical pressure probe methodology (Franks et al., 1995; Franks et al.,  
399 1998; Franks et al., 2001). We have therefore used an atomic force microscope (Beauzamy et al.,  
400 2015) to assess the amount of hydrostatic pressure required to cause indentation on guard cells  
401 and pavement cells. This methodology, which is not destructive, basically applies a non-  
402 penetrative indentation with an elastic probe on the sample surface (Beauzamy et al., 2015). The

403 applied force can be linearly deduced from the measured probe deformation, while the mechanical  
404 properties of the sample can be deduced from the applied force and sample surface deformation  
405 due to indentation. Turgor pressure is further deduced using established continuum mechanics  
406 equations of the inflated shell model (Beauzamy et al., 2015). This approach has been applied to  
407 epidermal cells in cotyledon (Verger et al., 2018), a system histologically similar to leaves, and in  
408 shoot apical meristem (Long et al., 2020). Following these two studies, we deduced turgor  
409 pressure using forces at depth ranges that minimize the influence of neighboring cells and of  
410 underlying cell layers or cavities (Malgat et al., 2016; Long et al., 2020).

411 The turgor pressure values deduced in the present study for wild-type *Arabidopsis* guard  
412 cells and pavement cells (close to 2 MPa and 1 MPa, respectively, in open stomata; Figure 6A),  
413 are within the range of values previously obtained by pressure probe applied to *Vicia faba* and  
414 *Tradescantia virginiana*, which ranged from 1 to 5 MPa for guard cells, and from 0.6 to 1 MPa for  
415 pavement cells (Franks et al., 1995; Franks et al., 1998). In all of these studies, pavement cells  
416 exhibited lower turgor pressure than guard cells. In *Arabidopsis*, the difference in turgor between  
417 guard cells and pavement cells observed in our experimental conditions is close to 0.8 MPa, which  
418 indicates that the osmolyte content of pavement cells was significantly lower than that of guard  
419 cells, by about  $\sim 330$  mOsm.L<sup>-1</sup>.

420 The AFM data did not reveal any significant difference in guard cell turgor between the wild-  
421 type and *atkc1-2*. In contrast, the turgor pressure of pavement cells was weaker in *atkc1-2* than in  
422 the wild-type, by about 0.15 MPa, i.e., by ca. 20% (Figure 6A). This decrease in turgor  
423 corresponds to a decrease in osmoticum concentration by about 60 mOsm.L<sup>-1</sup>. Such a difference  
424 is supported by the 40-60 mOsm.L<sup>-1</sup> difference in mannitol concentration required to induce  
425 epidermal cell plasmolysis in WT and *atkc1-2* plants as deduced from Figure 6B (the curves of the  
426 WT and *atkc1-2* mutant plants being shifted from each other by about 40-60 mOsm.L<sup>-1</sup>). Such  
427 differences are also consistent with the observation that the internal concentration of K<sup>+</sup> in  
428 epidermal strips was about 42 mM to 58 mM lower in the mutant plants (as computed from  
429 Figure 5 and Figure 8C, respectively, FW/DW ratio = 9). Thus, the decrease in pavement cell  
430 turgor revealed by microindentation in the *atkc1-2* mutant can be mainly ascribed to lower K<sup>+</sup>  
431 accumulation in these cells.

432 Because AtKC1 is a member of the Shaker K<sup>+</sup> channel family, its absence may disturb the  
433 steady-state accumulation of K<sup>+</sup> in diverse tissue types. The *atkc1-2* mutation has been found to  
434 affect neither whole root, whole shoot nor whole leaf K<sup>+</sup> contents (Jeanguenin et al., 2011) (Figure  
435 5). Thus, the decrease in leaf epidermal strip K<sup>+</sup> contents resulting from this mutation appears to  
436 be limited to this tissue. The observation that the *ProCER5:AtKC1* and *ProCYP96A4:AtKC1*  
437 constructs complemented the mutant defect in epidermal strip K<sup>+</sup> content (Figure 8C) and in

438 stomatal aperture control (Figure 8A-B) while the promoters *ProCER5* and *ProCYP96A4* are  
439 known to be essentially active in leaf epidermis (Pighin et al. 2004; Mustroph et al., 2009) (Figure  
440 S1) provides further evidence that both defects have their origin in the leaf epidermis and not in  
441 another plant tissue.

442 Membrane potential measurements indicated that the *atkc1-2* mutation resulted in a  
443 significant depolarization of pavement cells, by about 20 mV or 48 mV when the external solution  
444 contained 0.1 mM  $K^+$  or 10 mM  $K^+$ , respectively (Figure 7A). The magnitude of the depolarization  
445 induced by the 100-fold increase in the external  $K^+$  concentration was thus much larger in the  
446 mutant than in the WT pavement cells (Figure 7B-D). Altogether, these results provide evidence  
447 that the absence of AtKC1 functional expression impacted electrical features within the leaf  
448 epidermis. The decrease in membrane polarization resulting from the *atkc1-2* mutation is  
449 consistent with - and could result from or contribute to - the lower  $K^+$  content of mutant pavement  
450 cells (Figures 5, 6 and 8C). The increase in the sensitivity of the membrane potential to  $K^+$  external  
451 concentration, which indicates an increase in the membrane conductance to  $K^+$  in the mutant,  
452 when compared with the WT, is consistent with the fact that AtKC1 behaves as a negative  
453 regulator of inward Shaker channels (Jeanguenin et al., 2011). Indeed, AtKC1 does not form  
454 homotetrameric channels on its own, as indicated above, but can form heteromeric channels upon  
455 interaction with co-expressed inwardly rectifying Shaker channel subunits, leading to increased  
456 diversity in channel functional properties (Reintanz et al., 2002; DUBY et al., 2008; Geiger et al.,  
457 2009; Honsbein et al., 2009; Jeanguenin et al., 2011; Zhang et al., 2015; Wang et al., 2016). The  
458 activation potential of heteromeric channels associating AtKC1 to KAT1, KAT2 or AKT2 is shifted  
459 towards more negative values, when compared with KAT1, KAT2 or AKT2 homomeric channels  
460 (DUBY et al., 2008; Jeanguenin et al., 2011). Such negative regulation has been proposed to  
461 prevent  $K^+$  efflux (loss) when the membrane potential is less negative than the  $K^+$  equilibrium  
462 potential ( $E_K$ ) but more negative than the (homomeric) channel activation potential (DUBY et al.,  
463 2008; Jeanguenin et al., 2011).

464 Patch-clamp analysis revealed different types of current patterns amongst protoplasts  
465 derived from pavement cells recognizable by their size and shape, and in particular the fact that  
466 they did not possess chloroplasts. Thus, this analysis provides evidence that, within the leaf  
467 epidermis, cells that are neither guard cells nor trichomes (the latter cells being not digested by the  
468 enzyme cocktail in our experimental conditions) do not form a homogeneous tissue in terms of  
469 plasma membrane electrical properties. Evidence is available at the molecular level that the  
470 generic term of "pavement cells" actually belies a functionally heterogeneous population of cells,  
471 based on the criterion of gene expression markers. For instance, *PATROL1* is expressed in guard  
472 cells and only in the smallest of the immediately adjacent pavement cells. The other two

473 surrounding pavement cells do not express this gene to detectable levels. PATROL1 directs  
474 trafficking of certain proteins, including AHA1/OST2, a proton pump that is important for  
475 hyperpolarization of the plasma membrane (Merlot et al., 2007; Higaki et al., 2014). Moreover,  
476 single-cell gene transcriptomic profiling in the epidermis of Arabidopsis has revealed differences  
477 between pavement cells and basal trichome cells (also named socket or skirt cells) (Lieckfeldt et  
478 al., 2008; Schliep et al., 2010; Zhou et al., 2017). This diversity in gene expression, as well as the  
479 diversity in membrane electrical properties revealed by our patch-clamp recordings, might be  
480 related to the positional information sensed by the epidermal cells with respect to veins, trichomes  
481 and/or stomata.

482 None of the different types of current patterns displaying no time-dependent slowly activating  
483 component (Figure S3) is reminiscent of the activity of a cloned and functionally characterized ion  
484 channel. The situation is different for the protoplasts displaying a Shaker-like time-dependent  
485 activation (Figure 3). Indeed, the available transcriptome data (EMBL-EBI expression atlas) as  
486 well as *GUS* reporter gene analysis (Lacombe et al., 2000) indicate that, together with *AtKC1*, the  
487 Shaker gene *AKT2* is expressed in pavement cells. Thus, the Shaker-like slowly-activating weakly-  
488 inwardly rectifying current pattern (Figure 3) that was observed in about one-third or one-quarter  
489 (in the WT and the mutant, respectively) of the pavement cell protoplasts suggests that a  
490 significant part of the inward and outward currents was mediated by *AKT2* homomeric and  
491 heteromeric channels comprising, in WT plants, *AtKC1* subunits since both *AKT2* and *AKT2*-  
492 *AtKC1* channels have been shown to be weakly rectifying (Jeanguenin et al., 2011). The weak  
493 rectification of *AKT2* results from coexistence in the membrane of two populations of channels,  
494 one displaying activation by increasingly negative voltages and the other displaying an  
495 instantaneously activated non-rectifying ("leak-like") behavior, depending on the channel  
496 phosphorylation status (Michard et al., 2005a; Michard et al., 2005b). Such phosphorylation-  
497 controlled variations of the channel gating properties could also contribute to the diversity of  
498 plasma membrane electrical behavior amongst pavement cell protoplasts.

499 Comparison of the patch-clamp recordings in WT and *atkc1-2* pavement cell protoplasts did  
500 not provide evidence that the pavement cell diversity in plasma membrane electrical features was  
501 reduced by the mutation (Figures 3 and S3). The I-V curves derived for the WT and *atkc1-2*  
502 mutant protoplasts displaying a time-dependent slowly activating *AKT2*-like component are quite  
503 similar (Figure 3H). This suggests that it is not by affecting the time-dependent *AKT2*-like  
504 conductance that the *atkc1-2* mutation alters the pavement cell  $K^+$  content (Figure 5, 6 and 8) and  
505 the sensitivity of pavement cell membrane potential to  $K^+$  (Figure 7).

506 Altogether, these patch-clamp data leave the actual impact of the mutation on the  $K^+$   
507 conductance of (the different types of) pavement cells still elusive. Patch-clamp measurements on

508 protoplasts provide information about individual cell (protoplast) properties, while membrane  
509 potential measurements give access to data reflecting *in situ* (in the leaf apoplastic solution)  
510 integrated (within the leaf epidermis as a whole due to electrical connection through  
511 plasmodesmata) electrical properties. Such a difference, together with the large diversity in  $K^+$   
512 conductance amongst pavement cells and the fact that the present patch-clamp analysis has  
513 essentially taken into account the protoplasts whose membrane inward conductance appeared to  
514 be dominated by a time-dependent slowly-activating conductance (Figure 3), might explain that no  
515 significant difference between *atkc1-2* mutant and WT pavement cell protoplasts has been  
516 evidenced by this analysis.

517 It should also be noted that AtKC1 is known to play a role in exocytosis, besides its  
518 contribution to the regulation of inwardly rectifying Shaker channel activity. It interacts with the  
519 SNARE AtSYP121 (Honsbein et al., 2009), a vesicle-trafficking protein active at the plasma  
520 membrane and mediating vesicle fusion required for cellular homeostasis and growth (Geelen et  
521 al., 2002). Formation of tripartite complexes associating AtSYP121 to AtKC1, itself associated to  
522 the other Shaker subunit of the heteromeric channel, has been shown to confer voltage sensitivity  
523 to the contribution of AtSYP121 to vesicle fusion at the plasma membrane, rendering the secretion  
524 voltage dependent, a process proposed to couple  $K^+$  uptake to exocytosis and to maintain turgor  
525 pressure in growing plant cells (Honsbein et al., 2009; Grefen et al., 2015). Finally, screening tests  
526 using a split ubiquitin derived system suggest that AtKC1 might also interact with a ROP protein  
527 (Rho-of-Plant, a Rho GTPase) as well as a nitrate transporter (Obrdlik et al., 2004).

528 Fused to the *AtKC1* coding sequence, cell-type specific promoters directing expression in  
529 guard cells, or in both guard cells and pavement cells, or in trichomes only, did not complement  
530 the *atkc1* mutant stomatal phenotype, while complementation was observed with promoters  
531 directing expression in these three cell types together (Figure 8). Considering the whole set of  
532 observations, the simplest hypothesis is that AtKC1 contributes to non-autonomous guard cell  
533 control of stomatal aperture and that this contribution involves pavement cells and trichomes.

534 A salient finding from the patch-clamp recordings in pavement cell protoplasts is that, despite  
535 the observed diversity in cell membrane electrical properties (Figure 3 and Figure S3), pavement  
536 cells possess in common a rather weak level of rectification when compared to that displayed by  
537 guard cells (Figure 2). The model suggested by these results is thus that guard cells, with strong  
538 rectification of both inward and outward  $K^+$  conductances, are embedded in a layer of cells mostly  
539 displaying weak rectification. It is tempting to assume that this functional differentiation between  
540 pavement cells and guard cells renders the exchanges of  $K^+$  between these two types of cells  
541 immediately dependent on the guard cell membrane transport activity. The quasi-linearity of the  
542 current-voltage curve of pavement cells would allow that any change in  $K^+$  apoplastic



543 concentration due to uptake of this cation by - or release from - guard cells could modulate the  
544 efflux of  $K^+$  from - or influx into - pavement cells. In other words, due to their low level of  
545 rectification, pavement cells could be a permanent and immediately available  $K^+$  source or sink,  
546 depending on the demand of guard cells, in agreement with the model that guard cells play the  
547 dominant motor role in stomatal movements. Finally, the low level of rectification of pavement  
548 cells, which allows  $K^+$  exchanges in the whole range of membrane potentials, can also be  
549 hypothesized to facilitate  $K^+$  exchange/shuttling among the pavement cells themselves.

550 The mutant defect in stomatal movements observed *in planta* (Figure 1C) is not likely to  
551 directly result from altered control of  $K^+$  availability in the external solution (i.e., in the leaf  
552 epidermis apoplast) since impaired control of stomatal aperture was also observed *in vitro* in  
553 epidermal strips bathed in a solution containing a high concentration of  $K^+$  (Figure 1D, 4B, and  
554 8A), like that used in microindentation experiments (Figure 6A). Our results suggest that, when  
555 AtKC1 is functional, trichomes cooperate with adjacent epidermal cells in  $K^+$  homeostasis.  
556 *ProAtKC1*, as well as *ProCER5* and *ProCYP96A4*, which complemented the *atkc1-2* mutant, are  
557 all expressed in the ring of basal cells skirting the base of the trichome. The major class of  
558 transcripts detected in trichomes, basal and epidermal cells belong to transport and transport-  
559 associated proteins (Lieckfeldt et al., 2008), suggesting that these cells are particularly active in  
560 intra- and inter-cellular movements of solutes. Absence of *AtKC1* functional expression might  
561 affect  $K^+$  distribution between trichomes, basal cells and pavement cells, resulting in a reduction of  
562  $K^+$  accumulation in the latter cells.

563 In conclusion, the whole set of results supports the following causal chain: absence of *AtKC1*  
564 functional expression leads to a reduced steady-state  $K^+$  accumulation in pavement cells, and  
565 thereby in a decrease in the turgor of these cells. The weakened backpressure of the epidermal  
566 cells therefore surrenders to the opposing guard cell turgor, constitutively resulting in more open  
567 stomata. The present data provide genetic, molecular, and electrophysiological evidence that  
568 complex  $K^+$  distribution among several epidermal cell types contributes to stomatal aperture  
569 outcome. In conclusion, these data support the view that the entire epidermis should be regarded  
570 as a dynamic filter controlling stomatal aperture.

## 571 572 **MATERIALS AND METHODS**

### 573 574 **Plant Culture**

575  
576 *Arabidopsis thaliana* (Ws) plants were grown in a growth chamber, at 20°C, with a 8/16 h light/dark  
577 photoperiod (300  $\mu\text{mol photons}\cdot\text{m}^{-2}\cdot\text{s}^{-1}$ , white light from fluorescent tubes), at 70% RH (RH =

578 relative air humidity), in commercial compost. They were used for experiments when they were 6-  
579 weeks old and still not bolting.

### 581 **Stomatal aperture and transpiration measurements**

582  
583 Rosette transpirational water loss, preparation of leaf epidermal strips and measurements of  
584 stomatal aperture (in 30 mM KCl and 10 mM KOH-MES, pH 6.5) were performed as previously  
585 described (Hosy et al., 2003; Nieves-Cordones et al., 2012) . Stomatal aperture measurements  
586 were performed in triplicate on at least six epidermal strips from 6 different plants. To study the  
587 effect of increased mannitol concentration on stomatal aperture, epidermal strips were incubated  
588 in stomatal opening buffer containing 30 mM KCl and 10 mM KOH-MES, pH 6.5, under light for  
589 2 h and then transferred into dishes containing the same solution plus different concentrations of  
590 mannitol. Images were taken within 5 min incubation under a microscope (Olympus BH2) coupled  
591 to a color camera (Olympus Color View II). Displayed data are mean of at least 100 values per  
592 treatment and per mannitol concentration (when stated) for each plant genotype. All experiments  
593 were conducted in blind, *i.e.* genotypes unknown to the experimenter until data had been  
594 analyzed. Vital staining with neutral red at 0.02% (w/v) was performed to confirm the viability of  
595 guard cells and other epidermal cells in epidermal strips. For whole-plant transpiration assays,  
596 pots containing individually grown 6 week-old plants subjected to the same watering regime were  
597 sealed with a plastic film to prevent water loss from the substrate. The soil water content was  
598 initially adjusted to 2.5 g of H<sub>2</sub>O per g of dry soil. Evapo-transpirational water loss was then  
599 compensated by addition of equivalent amounts of water in order to maintain the water content at  
600 its initial value over a four-day period. Pots were weighed twice a day, at dusk and at dawn, for  
601 determination of transpirational water loss (in milliliters H<sub>2</sub>O per square centimeter of leaf and per  
602 hour). Foliar area was measured with ImageJ from images of rosettes. Stomatal conductance was  
603 measured on intact leaves with a diffusion porometer (AP4; Delta-T Devices).

### 605 **Patch-clamp recordings**

606  
607 WT and *atkc1-2 Arabidopsis thaliana* Ws plants were grown for 6 weeks in compost (individual  
608 containers) in a growth chamber (20°C, 65% relative humidity, 8 h/16 h light/dark, 250  $\mu\text{mol m}^{-2}\cdot\text{s}^{-1}$ ).  
609 Electrophysiological analyses on guard cell protoplasts were performed as previously described  
610 (Hosy et al., 2003; Lebaudy et al., 2008). Epidermal cell protoplasts were isolated by enzymatic  
611 digestion of leaf epidermal strips in darkness. The digestion solution contained 1 mM CaCl<sub>2</sub>, 2 mM  
612 ascorbic acid, 1 mM Mes-KOH (pH 5.5), Onozuka RS cellulase (1% w/v, Duchefa Biochemie,

Haarlem, Netherlands), and Y-23 pectolyase (0.1% w/v, Seishin Pharmaceutical, Tokyo, Japan). The osmolarity was adjusted to 500 mosM with D-mannitol. The epidermal strips were digested for 35 min at 27°C. Filtration through 50- $\mu$ m mesh allowed recovery of protoplasts. The filtrate was rinsed four times with two volumes of conservation buffer: 100 mM potassium glutamate, 10 mM CaCl<sub>2</sub>, 10 mM HEPES, the osmolarity being adjusted to 520 mOsm with D-mannitol and the pH to 7.5 with KOH. The protoplast suspension was allowed to sediment and then kept on ice in darkness in the conservation buffer, which was also used as external solution for the sealing step. Patch-clamp pipettes were pulled (P07, DMZ-Universal Puller, Zeitz-Instruments, Germany) from borosilicate capillaries (GC150TF-7.5, Phymep, France). The pipette solution contained 1 mM CaCl<sub>2</sub>, 5 mM EGTA, 0.5 mM MgCl<sub>2</sub>, 100 mM potassium glutamate, 2 mM Mg-ATP, 20 mM HEPES. The osmolarity of the solution was adjusted to 540 mOsm with D-mannitol and the pH was adjusted to 7.5 with KOH (final K<sup>+</sup> concentration assayed by flame spectrophotometry: ca. 140 mM). Under these conditions, the pipette resistance was about 18 M $\Omega$ . Seals with resistance > 1 G $\Omega$  were used for electrophysiological analyses. The bath solution contained, except when otherwise mentioned, 100 mM potassium glutamate, 0.1 mM CaCl<sub>2</sub>, 10 mM HEPES, the osmolarity being adjusted to 520 mOsm with D-mannitol and the pH to 7.5 with KOH (final K<sup>+</sup> concentration: 105 mM, assayed by flame spectrophotometry). Whole-cell recordings were obtained using an Axon Instruments Axopatch 200B amplifier. pCLAMP 8.2 software (Axon Instruments, Foster City, CA) was used for voltage pulse stimulation, online data acquisition, and data analysis. The voltage protocol consisted of stepping the membrane potential from -40 mV (holding potential) to +80 mV or -205 mV, or from +25 mV (holding potential) to either +130 mV or -140 mV, in 15 mV steps. Liquid junction potentials at the pipette/bath interface were measured and corrected.

### Membrane potential recordings in pavement cells

Rosette leaves from WT and *atkc1-2* mutant plants grown in hydroponics for 3 weeks (1/5 Hoagland solution) were excised and immobilized in a 1-mL chamber. The external solution contained 5 mM MES (2-(N-Morpholino) ethanesulphonic acid), 0.1 mM KCl, 0.1 mM CaCl<sub>2</sub> and 0.1 mM NaCl, brought to pH 6.0 with Ca(OH)<sub>2</sub>. The leaf was bathed for at least 30 minutes in the perfusion solution before cell impalement. Impalement micro-electrodes were pulled from borosilicate glass capillaries (1B120F-4, World precision instruments, <http://www.wpiinc.com>) and showed a diameter of approximately 0.5  $\mu$ m at the tip. Glass microelectrodes were fixed to electrode holders containing an Ag/AgCl pellet and connected to a high-impedance amplifier (model duo 773; World precision instruments). Impalement and reference electrodes were filled

648 with 200 mM KCl. To impale leaf pavement cells, the micro-electrode was approached to the leaf  
649 surface with a motorized micro-manipulator (Narishige MM-89, <http://narishige-group.com>) and  
650 impalements were carried out with a one-axis oil hydraulic micromanipulator (Narishige MO-10).  
651 The precise penetration of the micro-electrode into pavement cells was visually followed with an  
652 inverted microscope.

### 653 **Atomic force microscopy**

654  
655  
656 AFM determination of turgor pressure in the leaf epidermis was performed as in Beuzamy et al.  
657 (2015) with modifications. Specifically, 1×1 cm leaf segments were fixed in Petri-dishes by double-  
658 sided tape and microtube tough-tags (Diversified Biotech) with the abaxial face up. Adaxial  
659 trichomes were removed by tweezers to facilitate tape fixation. Leaf segments were incubated in  
660 the stomata opening buffer (see above) under light for at least 2 hours before being mounted onto  
661 a BioScope Catalyst AFM (Bruker). A spherical-tipped AFM cantilever with 400 nm tip radius and  
662 42 N/m spring constant was used for the measurements (SD-SPHERE-NCH-S-10, Nanosensors);  
663 a spherical tip was used to avoid the cell wall puncture that often occurs upon usage of a more  
664 standard sharp pyramidal tip. One to 2 μm-deep indentations were made along the topological  
665 skeletons of epidermal cells to ensure relative normal contact between the probe and sample  
666 surface. At least 3 indentation positions were chosen for each cell, with each position  
667 consecutively indented 3 times, making at least 9 indentation force curves per cell. Cell recordings  
668 of AFM force curves were performed with the NanoIndentation plugin for ImageJ (<https://fiji.sc/>) as  
669 described in (Long et al. 2020). Parameters for turgor deduction were generated as follows. The  
670 cell wall elastic modulus and apparent stiffness were calculated from each force curve following  
671 Beuzamy et al. (2015). To minimize the effect of neighboring and underlying cells (Malgat et al.,  
672 2016; Long et al., 2020), we used a force range of 1-10% of maximal force for modulus and 75-  
673 99% of maximal force for cell stiffness, which typically correspond to depths in the ranges 10-100  
674 nm and 400-500 nm, respectively. Cell surface curvature was estimated from AFM topographic  
675 images, with the curvature radii fitted to the long and short axes of small cells or along and  
676 perpendicular to the most prominent topological skeleton of heavily serrated pavement cells.  
677 Turgor pressure was further deduced from each force curve (4 iterations) with the simplified  
678 hypothesis that the surface periclinal cell walls of leaf epidermis have a constant thickness, at 200  
679 nm, and cell-specific turgor pressure is retrieved by averaging all turgor deductions per cell.

## 681 **Plasmolysis assays**

682  
683 Epidermal strips were peeled, fixed on glass slides, and bathed in solutions differing in mannitol  
684 concentration. The percentage of strips displaying plasmolysis within 5 min incubation was  
685 determined using a microscope.

## 687 **Tissue K<sup>+</sup> content**

688  
689 Leaf margins were isolated by obtaining 2 mm razor-cut bands, which were enriched for  
690 hydathodes. Leaf epidermis was obtained by peeling abaxial epidermis with forceps. K<sup>+</sup> contents  
691 were determined in dried samples by flame spectrometry (SpectrAA 220 FS, Varian,  
692 <http://www.varianinc.com/>), after ionic extraction (sample incubation for 2 d in 0.1 N HCl).

## 694 **Complementation of *atkc1-2* mutant plants and promoter analyses**

695  
696 Mutant isolation and generation of transgenic plants expressing *AtKC1* under its native promoter  
697 has been described elsewhere (Jeanguenin et al., 2011). For guard cell specific complementation  
698 of *atkc1-2* mutant plants, *AtKC1* and *AtKC1-DN* cDNAs were expressed under the *KAT1* promoter  
699 in pCambia1301 vector (Hajdukiewicz et al., 1994). *AtKC1-DN* has been described previously  
700 (Jeanguenin et al., 2011) and contained two pore residue mutations (G291R and Y292R) that  
701 rendered it a dominant-negative channel subunit. For other indicated cell-specific expression of  
702 *AtKC1* we cloned the previously characterized genomic regions upstream of the first ATG from the  
703 loci *CER5*, *OCT3*, *GL2*, *At1G66460* and *FMO1* in the pCambia1301 vector to drive *AtKC1*  
704 expression. For expression pattern analyses, the same upstream regions were also cloned in  
705 pGWB3 using Gateway cloning (Nakagawa et al., 2007) to drive *GUS* expression in wild-type  
706 transformed plants, except *ProOCT3:GUS* lines that were kindly gifted by Isabell Kufner and  
707 described elsewhere (Kufner and Koch, 2008). For previously uncharacterized promoters  
708 (*ProCYP96A4* and *ProKCS19*), the inter-genomic regions located between the first ATG and the  
709 3'-end of the corresponding upstream loci were amplified. Floral dip method was used to transfect  
710 *Arabidopsis* plants (Clough and Bent, 1998). Transformed lines were verified by RT-PCR on RNA  
711 extracted from leaves of individual T1 plants, and T2 progeny homozygous for the transgene were  
712 selected based on true segregation of the linked hygromycin resistance marker of pCambia1301.  
713 Experiments were conducted on T3 homozygous plants.

## 715 **Guard cell protoplast preparation for gene expression analysis**

716

717 About 30-35 fully expanded rosette leaves were kept in cold water and in the dark. Main veins of  
718 leaves were removed using a scalpel. Leaf pieces were blended 3 times for 45 s at full speed, the  
719 yielded mixture was put over a nylon mesh and rinsed with cold distilled water. The epidermis  
720 fragments recovered from the 75 µm nylon mesh were digested for 30-45 min at 25°C with gentle  
721 shaking (140 rpm) in an enzyme solution (0.7% Calbiochem cellulysin, 0.1% PVP 40, 0.25% BSA,  
722 0.5 mM ascorbic acid, 45% distilled water and 55% solution containing sorbitol 560 mmol/kg, 5  
723 mM MES, 0.5 mM CaCl<sub>2</sub>, 0.5 mM MgCl<sub>2</sub>, 0.5 mM ascorbic acid, pH 5.5 with Tris). Translation  
724 inhibitor (100 mg/L Cordycepin, C3394-Sigma) and transcription inhibitor (33 mg/L Actinomycin D,  
725 A1410- Sigma) were also added to the digestion mixture. The digestion process was followed  
726 under a microscope (Olympus BH2), to check that "intact" guard cells were still present *in situ* in  
727 the digested epidermis at the end of the enzymatic treatment. The undigested fraction was  
728 recovered by filtration through 40 µm nylon mesh, rinsed with basic solution and stored at -80 °C.

729

### 730 **Gene expression analysis by RT-qPCR**

731

732 Total RNA extraction, synthesis of first-strand cDNAs and quantitative RT-PCR procedures were  
733 performed as described elsewhere (Cuellar et al., 2010). Primers used for real time qRT-PCR  
734 were designed using PRIMER3 (<http://frodo.wi.mit.edu>) (Table S2). All amplification plots were  
735 analysed with an Rn threshold (normalised reporter) of 0.2 to obtain CT (threshold cycle) values.  
736 Standard curves for *AtKC1*, *KAT1*, *KAT2* and *GORK* were obtained from dilution series of known  
737 quantities of corresponding cDNA fragments used as templates. Standard curves were used to  
738 calculate the absolute numbers of tested cDNA molecules in each cDNA sample, and these  
739 values were then normalised against corresponding housekeeping gene signals. Four  
740 housekeeping genes *EF1alpha*, *TIP41*, *PDF2* and *MXC9.20* (Czechowski et al., 2005) were used  
741 to calculate a normalization factor with the online algorithm "geNorm" (<https://genorm.cmgg.be/> ).

742

## 743 Expression analyses by GUS staining

744  
745 GUS staining of leaves from 6-week-old transgenic plants expressing the  $\beta$ -glucuronidase (GUS)  
746 reporter gene under the control of the promoters listed in Figure S1 was performed as described  
747 elsewhere (Lagarde et al., 1996). Similar expression patterns were obtained in three independent  
748 transgenic lines for each promoter.

## 749 Statistical analysis

750  
751 Statistical analysis was performed using the two-tailed Student's *t* test, Analysis of Variance  
752 (ANOVA) and Tukey's post-hoc test as indicated with Statistix V.8 software for Windows. The  
753 results are shown in Supplemental Data Set S1.

## 754 Accession Numbers

755  
756 Sequence data from this article can be found in the TAIR (Arabidopsis) database under accession  
757 numbers: *AtKC1* (At4G32650), *KAT1* (AT5G46240), *CER5* (At1G51500), *OCT3* (At1G16390),  
758 *GL2* (At1G79840), *Uncharacterized Protein Kinase* gene (At1G66460), *FMO1* (At1G19250),  
759 *CYP96A4* (At5G52320) and *ProKCS19* (At5G04530).

## 760 Supplemental Data

761  
762 **Supplemental Figure S1.** Expression patterns driven by the *AtKC1* promoter and by other  
763 selected cell-specific promoters in leaf epidermis.

764 **Supplemental Figure S2.** Stomatal density in wild-type and *atkc1-2* leaves (abaxial side).

765 **Supplemental Figure S3.** Example of non Shaker-like channel activities in pavement cell  
766 protoplasts from *Arabidopsis thaliana* wild type and *atkc1-2* mutant plants (Ws ecotype).

767 **Supplemental Figure S4.** Expression of *AtKC1* and *AtKC1-DN* under the *KAT1* promoter.

768 **Supplemental Figure S5.** Expression patterns driven by *AtKC1* promoter and by other selected  
769 cell-specific promoters in abaxial leaf epidermis and trichomes.

770 **Supplemental Figure S6.** The *atkc1-2* mutation does not affect trichome density in wild type and  
771 *atkc1-2* plants.

772 **Supplemental Table S1.** Cell-specific expression level of the genes selected in complementation  
773 experiments (Figure 8) obtained from eFP browser site. Supports Figure 8.

774 **Supplemental Table S2.** Primer list.

775 **Supplemental Data Set S1.** Statistical analysis results.

## 778 **ACKNOWLEDGEMENTS**

779 We thank Isabell Kufner for providing *ProOCT3:GUS* lines. This work was supported by the  
780 Alfonso Martin Escudero Foundation (to M.N.-C.), the Marie Curie Programme (grant no. 272390  
781 FP7–IEF to M.N.-C.), and the European Research Council (PhyMorph #307387 to A.B.).  
782

## 783 **AUTHOR CONTRIBUTIONS**

784 M. N.-C. carried out the mutant phenotyping, cell-specific complementation experiments and  
785 membrane potential recordings by microelectrode impalement. F. A. performed the gene  
786 expression and guard cell complementation analyses. G. D. carried out the mutant phenotyping  
787 experiments and the epidermal plasmolysis assays. K. M., A. V., T. S. and F. G. identified the  
788 mutant phenotype and conducted the first transpiration analyses. M. B., E. H. and A.-A. V.  
789 carried out the patch-clamp analyses on guard cell and pavement cell protoplasts. M. N.-C., A.  
790 V. and I. G. performed the stomatal aperture measurements. I. C., J. L. and T.S. contributed to the  
791 project conception. I. G. supervised the gene expression, mutant phenotyping and  
792 complementation experiments. Y.L. performed the atomic force microscopy measurements; Y.L.  
793 and A.B. designed the AFM experiments and analyzed the AFM data. H. S. and J.-B. T. jointly  
794 supervised the whole project. M. N.-C., H. S., J.-B. T., and J. L. and A.-A. V wrote the manuscript.  
795



796 **Table 1. Summary of the results presented in Figure S1 (expression pattern) and Figure 8A**  
 797 **(stomatal aperture)**  
 798

AtKC1 expression in	Promoter								
	<i>Pro</i> <i>AtKC1</i>	<i>Pro</i> <i>CER5</i>	<i>Pro</i> <i>CYP96A4</i>	<i>Pro</i> <i>KCS19</i>	<i>Pro</i> <i>OCT3</i>	<i>Pro</i> <i>KAT1</i>	<i>Pro</i> <i>GL2</i>	<i>Pro</i> <i>At1G66460</i>	<i>Pro</i> <i>FMO1</i>
<i>Guard cells</i>	+	+	+	+	+	+	-	-	-
<i>Pavement cells</i>	+	+	+	+	+	-	-	-	-
<i>Trichomes</i>	+	+	+	-	-	-	+	+	-
<i>Hydathodes</i>	+	+	-	-	+	-	-	-	+
Stomatal aperture similar to that in WT plants	Yes	Yes	Yes	No	No	No	No	No	No

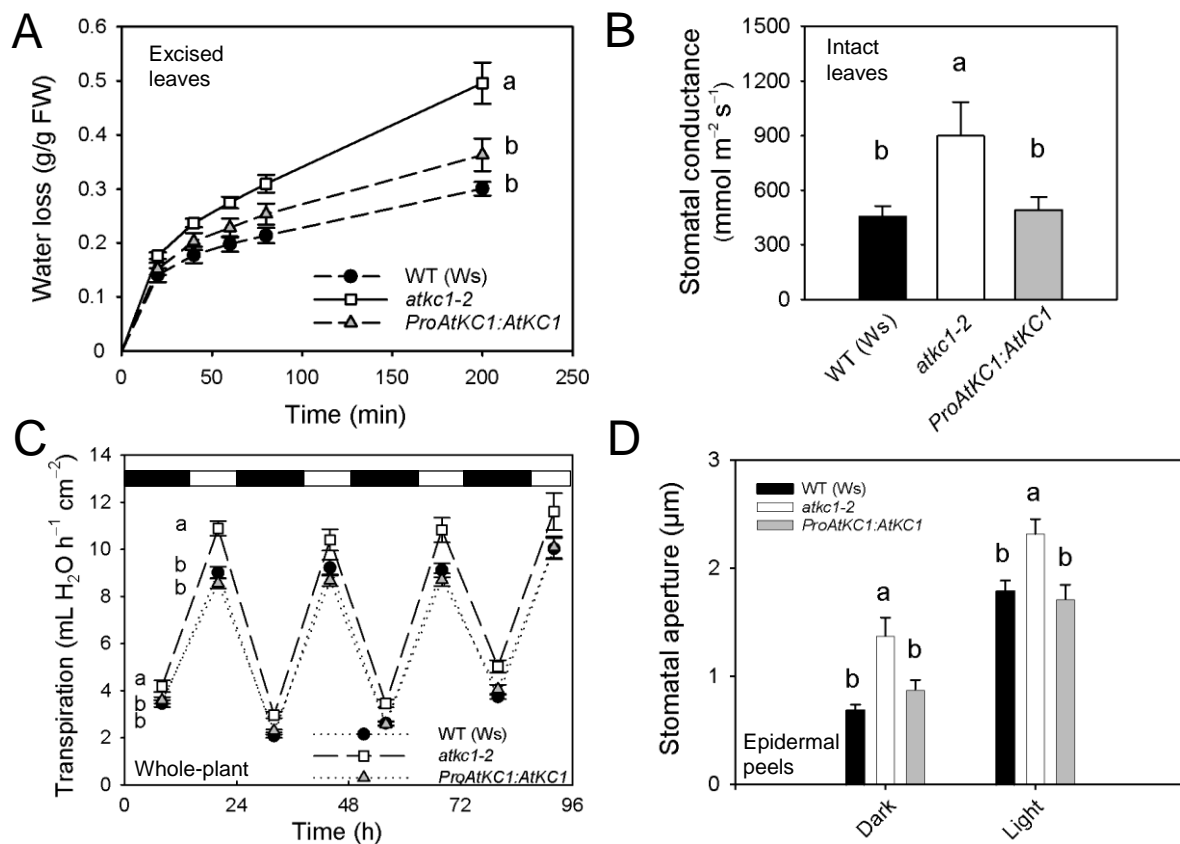


**Figure 1.** Impaired control of stomatal aperture and transpirational water loss in *atkc1-2* mutant plants. **(A)** Transpirational water loss from excised leaves. The second leaf was excised from wild-type (WT, Ws ecotype), *atkc1-2* and *ProAtKC1:AtKC1*-complemented *atkc1-2* plants. Excised leaf water loss was deduced from the decrease in leaf weight. **(B)** Leaf water conductance measured on intact leaves with a porometer. **(C)** Transpiration rates in whole-plant assays. **(D)** Stomatal aperture in WT, *atkc1-2* and *ProAtKC1:AtKC1*-complemented *atkc1-2* plants. Before stomatal aperture measurements, epidermal strips were kept in the dark for 2 h (Dark treatment) or in dark for 2 h, followed by 2 h in the light (Light treatment) in a 40 mM K<sup>+</sup> solution. **(A) to (D)** Means  $\pm$  SE. In **(A)**, **(B)** and **(C)**,  $n = 5$ ,  $9$  and  $11$ , respectively; in **(D)**,  $n = 6$  values, each value corresponding to  $\sim 100$  stomata. Letters depict significant group values after analysis of variance (ANOVA) and Tukey's post-hoc test. In **C**, for the statistical analysis, the data obtained during the four consecutive days were pooled, taking into account the corresponding day cycle.

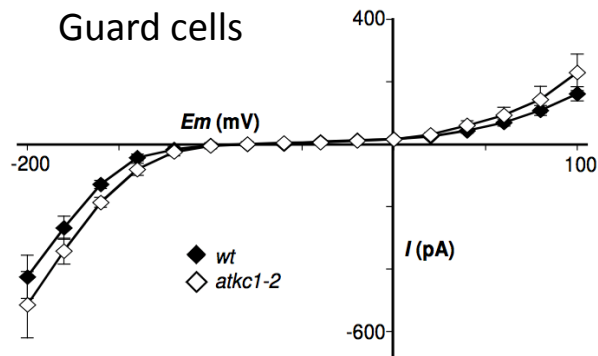


**Figure 2.** Shaker-like  $K^+$  channel activity in guard cells from wild type and *atkc1-2* mutant plants (Ws ecotype). Guard cell protoplast current/voltage relationships. Means  $\pm$  SE;  $n = 8$  and  $10$  for the wild type and mutant genotypes, respectively. External K-glutamate concentration was  $100$  mM.

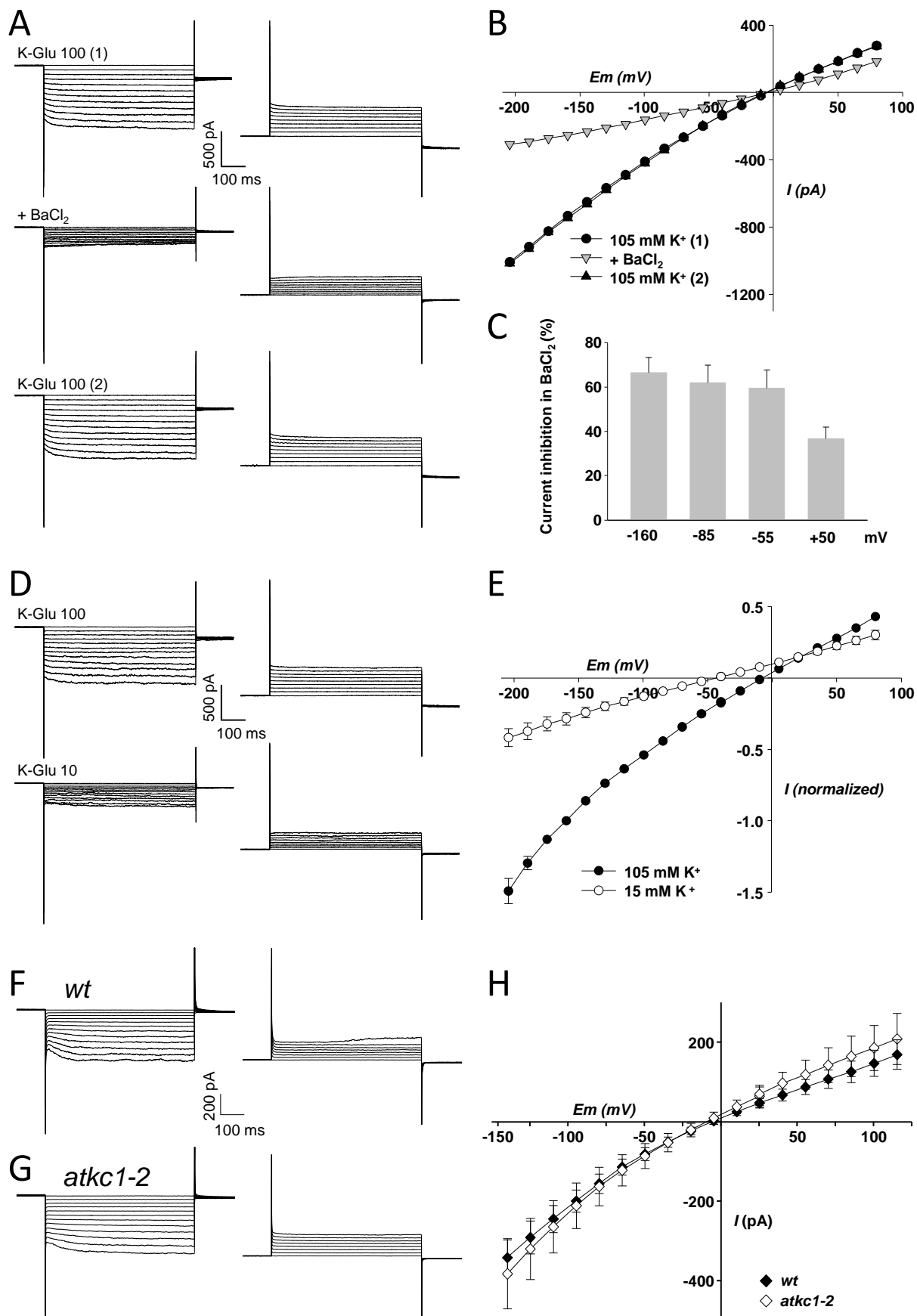


**Figure 3.** Weakly inwardly-rectifying K<sup>+</sup> channel activity in pavement cells from wild type and *atkc1-2* mutant plants (Ws ecotype). **(A-C)** Typical weakly inwardly-rectifying K<sup>+</sup> currents recorded in pavement cell protoplasts and their blockage by 10 mM external BaCl<sub>2</sub>.

**(A)** Example of inward and outward current traces (right and left panels, respectively), recorded in the presence of 100 mM K-glutamate (total K<sup>+</sup> concentration: 105 mM) and successively before BaCl<sub>2</sub> addition (top panels), in the presence of BaCl<sub>2</sub> (middle panel) and after BaCl<sub>2</sub> rinse (lower panels). **(B)** Corresponding current/voltage relationships. **(C)** Current inhibition in the presence of BaCl<sub>2</sub> at negative and positive voltages. Means ± SE; n = 7. **(D)** and **(E)** Effect of change in external K-glutamate concentration on the weakly inwardly rectifying currents in pavement cell protoplasts. **(D)** Example of inward and outward current traces (right and left panels, respectively) recorded successively in 100 mM K-glutamate (top panels) and 10 mM K-glutamate (lower panels; total K<sup>+</sup> concentration: 15 mM). **(E)** Current/voltage relationships in the two external K-glutamate conditions. Currents were normalized in each protoplast by the current value obtained in 100 mM K-glutamate at -160 mV. Means ± SE; n = 7. **(F)** and **(G)** Representative inward and outward (right and left panels, respectively) Shaker-like K<sup>+</sup> current traces in wild type **(F)** and *atkc1-2* **(G)** pavement cell protoplasts. **(H)** Pavement cell protoplast Shaker-like current/voltage relationship in wild type and *atkc1-2* mutant plants. External K-glutamate concentration: 100 mM. Means ± SE; n = 8 for both the wild type and the mutant genotypes. The concentration of K<sup>+</sup> (essentially as glutamate salt) in the pipette solution and in the bath solution was 140 and 105 mM, respectively, which results in a K<sup>+</sup> equilibrium potential close to -7 mV.

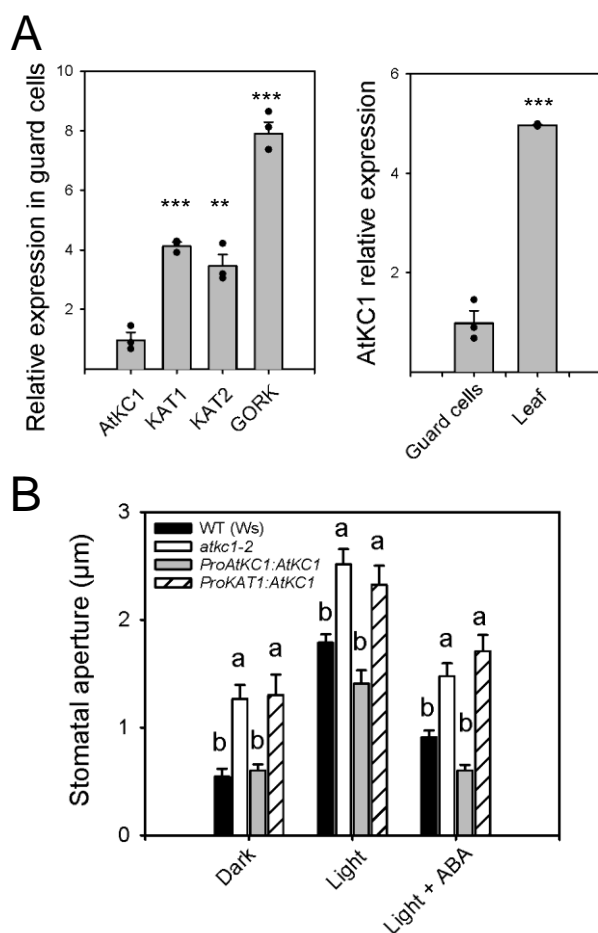


**Figure 4.** The defect in stomatal aperture displayed by the *atkc1-2* mutant does not result from loss of *AtKC1* expression in guard cells.

**(A)** Relative expression of *AtKC1* compared to that of other Shaker channels in guard cells (left panel) and relative expression of *AtKC1* in guard cells compared to that in leaves (right panel). Expression levels determined by RT qPCR experiments.

**(B)** Stomatal aperture in wild type plants (WT), in *atkc1-2* mutant plants and in *atkc1-2* mutant plants transformed with either the complementing *ProAtKC1:AtKC1* construct (see Figure 1) or with a construct, *ProKAT1:AtKC1*, rendering *AtKC1* expression dependent on the activity of the promoter of *KAT1*, a Shaker channel gene whose expression in guard cells is specific of this cell type in leaf epidermis (see also supplemental Figure S4). "Dark" and "Light" treatments: stomatal aperture was measured under dark or light as described in Figure 1D. "Light + ABA" treatment: 10  $\mu$ M ABA was applied for 2 h to light-treated strips before stomatal aperture measurement.

**(A)** and **(B)** Means  $\pm$  SE. For **(A)**,  $n = 3$  pools of 5-6 plants, and \*\* and \*\*\* denote  $p < 0.01$  and  $< 0.001$  in a two-tailed Student's T-test (comparison *AtKC1* expression to that of *KAT1*, *KAT2* or *GORK*, left panel, and *AtKC1* expression in guard cells vs *AtKC1* expression in leaves, right panel). For **(B)**,  $n = 6-10$  values, each value corresponding to  $\sim 60$  stomata. Letters depict significant group values after analysis of variance (ANOVA) and Tukey's post-hoc test.

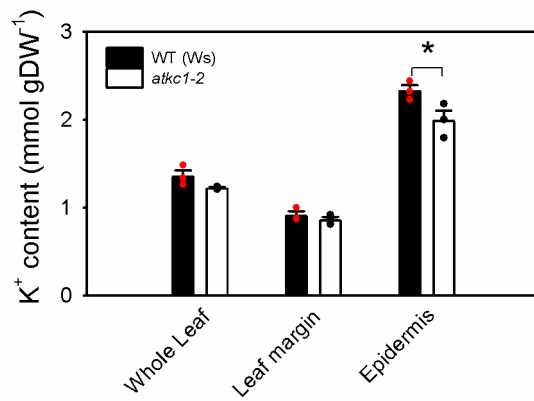


**Figure 5.** Disruption of *AtKC1* leads to reduced K<sup>+</sup> contents in leaf epidermis. K<sup>+</sup> contents in whole leaf, leaf margin and leaf epidermis in wild type and *atkc1-2* mutant plants. Means  $\pm$  SE; n = 3 pools, each one obtained from 9 leaves (\*,  $p < 0.05$ , using two-tailed Student's T-test).

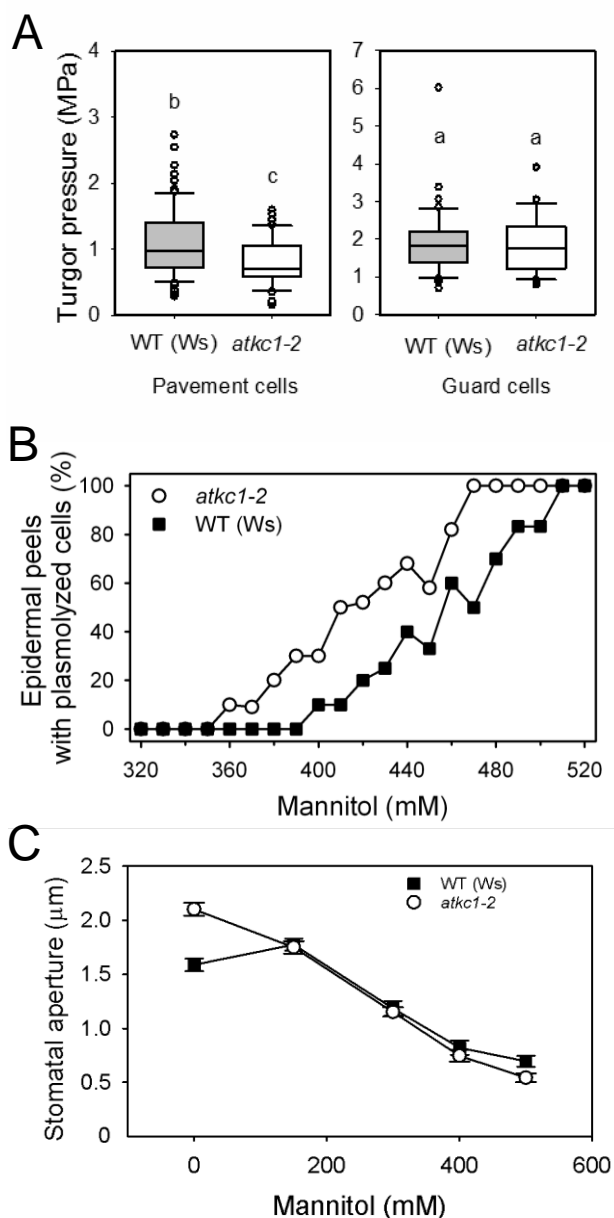


**Figure 6.** Disruption of *AtKC1* leads to reduced turgor pressure in pavement cells but not in guard cells. **(A)** Boxplots depicting turgor pressure values obtained with atomic force microscopy in wild-type and *atkc1-2* pavement cells (left panel) and guard cells (right panel). Upper and lower whiskers : 1.5 times the IQR (first to third interquartile range), border of the boxes: first and third quartile, central line: median. Letters depict different group values after Student T-test ( $p < 0.05$ ). For guard cells,  $n = 46$  for the wild type genotype and 32 for the *atkc1-2* mutant genotype. For pavement cells,  $n = 86$  for the wild type and 51 for the mutant genotype. **(B)** Disruption of *AtKC1* results in decreased osmotic pressures in leaf epidermis as deduced from plasmolysis curves obtained by measuring the percentage of epidermal strips displaying plasmolyzed cells when bathed for 5 min in the presence of mannitol. Ten to 12 strips were examined for each genotype and mannitol concentration. **(C)** Effect on stomatal aperture of adding mannitol to the solution bathing epidermal strips from wild type or *atkc1-2* mutant plants.  $n = 92-120$  from 6 leaves for each mannitol concentration and genotype.



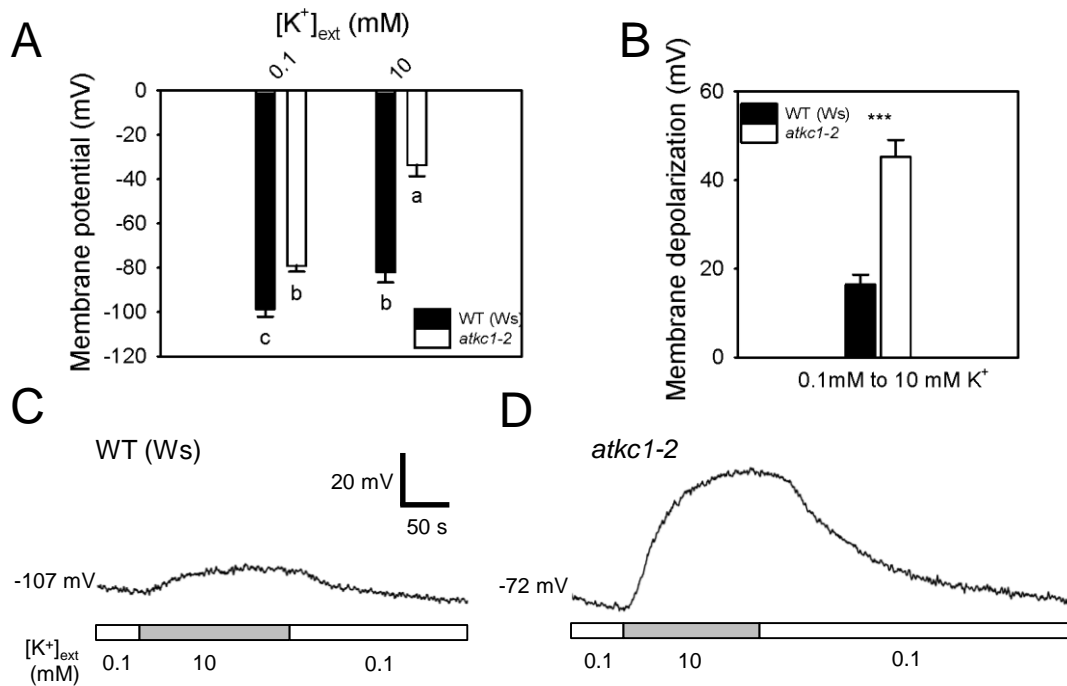


**Figure 7.** The *atkc1-2* mutation results in membrane depolarization in pavement cells and in an increased sensitivity of the membrane potential to the external concentration of K<sup>+</sup>. **(A)** Membrane potentials recorded in WT and *atkc1-2* pavement cells bathed in 0.1 mM or 10 mM K<sup>+</sup>. **(B)** Membrane depolarizations induced by the increase in external K<sup>+</sup> concentration from 0.1 mM to 10 mM. Each value corresponded to the difference in the membrane potential that was observed when the external K<sup>+</sup> concentration was increased from 0.1 mM to 10 mM K<sup>+</sup> within the same cell. **(C)** Representative trace of a WT pavement cell showing membrane depolarization and repolarization due to changes in external K<sup>+</sup> concentration. **(D)** Representative trace of an *atkc1-2* pavement cell subjected to the same protocol as in **(C)**. White and gray bars depict the periods where the external K<sup>+</sup> concentration was 0.1 mM and 10 mM, respectively. In **(A)** and **(B)**, means ± SE are shown. n = 14 cells from five different plants for WT and n = 14 cells from three different plants for *atkc1-2*. Letters depict significant group values after analysis of variance (ANOVA) and Tukey's post-hoc test. \*\*\* denotes p < 0.001 in a two-tailed Student's T-test.

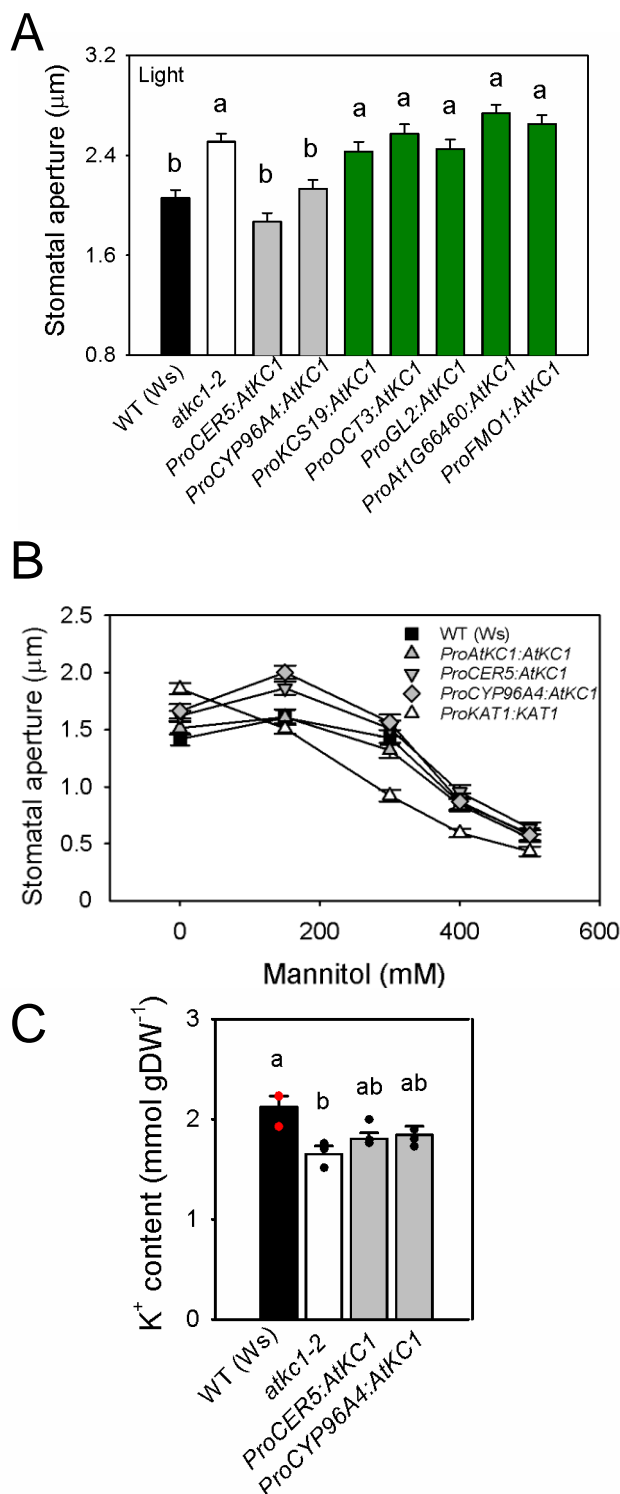


**Figure 8.** Restoration of wild-type stomatal features in the *atkc1-2* mutant requires *AtKC1* expression in pavement cells and trichomes.

**(A)** Stomatal aperture under light in wild-type *Arabidopsis* plants (Ws ecotype, black bar), in *atkc1-2* mutant plants (white bar) and in *atkc1-2* mutant plants transformed with a construct allowing expression of *AtKC1* under control of one of the following promoters: *ProCER5*, *ProCYP96A4*, *ProKCS19*, *ProOCT3*, *ProGL2*, *ProAt1G66460* and *ProFMO1* (expression patterns of these promoters: see Table 1 and Supplemental Figures 1 and 5). Grey bars and dark green bars: transformed plants with rescued or non-rescued stomatal phenotype, respectively. Stomatal aperture was measured following the same procedure as in Figure 6D.

**(B)** Stomatal aperture in epidermal strips bathed in mannitol solutions. Transformed lines identified in **(A)** as displaying stomatal aperture values similar to that of wild-type plants (transforming constructs: *ProAtKC1:AtKC1*, *ProCER5:AtKC1* and *ProCYP96A4:AtKC1*) also behaved like wild-type plants in response to added mannitol (showing a non-monotonous sensitivity to mannitol concentration). In contrast, the transgenic line *ProKAT1:AtKC1*, shown in **(A)** to display a stomatal aperture similar to that of *atkc1-2* mutant plants, also displayed a monotonous decrease in stomatal aperture in response to increased mannitol concentration, and thus behaved like *atkc1-2* mutant plants (see Figure 6C).

**(C)** Leaf epidermis K<sup>+</sup> content in wild type plants, in *atkc1-2* mutant plants and in *atkc1-2* mutant plants transformed with the *ProCER5:AtKC1* and *ProCYP96A4:AtKC1* complementing constructs.

**(A)** to **(C)** Means ± SE. In **(A)** and **(B)**, n = 94-131 stomata from 6 leaves. In **(C)**, n = 3 pools of samples, each one obtained from 9 leaves. In **(A)** and **(C)**, letters depict significant group values after analysis of variance (ANOVA) and Tukey's post-hoc test.

804  
805  
806  
807  
808  
809  
810  
811  
812  
813  
814  
815  
816  
817  
818  
819  
820  
821  
822  
823  
824  
825  
826  
827  
828  
829  
830  
831  
832  
833  
834  
835  
836

## REFERENCES

- Bauer, H., Ache, P., Lautner, S., Fromm, J., Hartung, W., Al-Rasheid, K.A., Sonnewald, S., Sonnewald, U., Kneitz, S., Lachmann, N., Mendel, R.R., Bittner, F., Hetherington, A.M., and Hedrich, R.** (2013). The stomatal response to reduced relative humidity requires guard cell-autonomous ABA synthesis. *Curr. Biol.* **23**: 53-57.
- Beuzamy, L., Derr, J., and Boudaoud, A.** (2015). Quantifying hydrostatic pressure in plant cells by using indentation with an atomic force microscope. *Biophys. J.* **108**: 2448-2456.
- Blatt, M.R.** (2000). Cellular signaling and volume control in stomatal movements in plants. *Annu. Rev. Cell. Dev. Biol.* **16**: 221-241.
- Britto, D.T., Coskun, D., and Kronzucker, H.J.** (2021). Potassium physiology from Archean to Holocene: A higher-plant perspective. *J. Plant Physiol.* **262**: 153432.
- Clough, S.J., and Bent, A.F.** (1998). Floral dip: a simplified method for *Agrobacterium*-mediated transformation of *Arabidopsis thaliana*. *Plant J.* **16**: 735-743.
- Cuellar, T., Pascaud, F., Verdeil, J.L., Torregrosa, L., Adam-Blondon, A.F., Thibaud, J.B., Sentenac, H., and Gaillard, I.** (2010). A grapevine Shaker inward K<sup>+</sup> channel activated by the calcineurin B-like calcium sensor 1-protein kinase CIPK23 network is expressed in grape berries under drought stress conditions. *Plant J.* **61**: 58-69.
- Czechowski, T., Stitt, M., Altmann, T., Udvardi, M.K., and Scheible, W.R.** (2005). Genome-wide identification and testing of superior reference genes for transcript normalization in *Arabidopsis*. *Plant Physiol.* **139**: 5-17.
- Daram, P., Urbach, S., Gaymard, F., Sentenac, H., and Chérel, I.** (1997). Tetramerization of the AKT1 plant potassium channel involves its C-terminal cytoplasmic domain. *EMBO J.* **16**: 3455-3463.
- Duby, G., Hosy, E., Fizames, C., Alcon, C., Costa, A., Sentenac, H., and Thibaud, J.B.** (2008). AtKC1, a conditionally targeted Shaker-type subunit, regulates the activity of plant K<sup>+</sup> channels. *Plant J.* **53**: 115-123.
- Franks, P.J., Cowan, I.R., and Farquhar, G.D.** (1998). A study of stomatal mechanics using the cell pressure probe. *Plant Cell Environ.* **21**: 94-100.
- Franks, P.J., Buckley, T.N., Shope, J.C., and Mott, K.A.** (2001). Guard cell volume and pressure measured concurrently by confocal microscopy and the cell pressure probe. *Plant Physiol.* **125**: 1577-1584.

- 837 **Franks, P.J., Cowan, I.R., Tyerman, S.D., Cleary, A.L., Lloyd, J., and Farquhar, G.D.** (1995).  
838 Guard-cell pressure aperture characteristics measured with the pressure probe. *Plant Cell*  
839 *Environ.* **18**: 795-800.
- 840 **Geelen, D., Leyman, B., Batoko, H., Di Sansebastiano, G.P., Moore, I., and Blatt, M.R.** (2002).  
841 The abscisic acid-related SNARE homolog NtSyr1 contributes to secretion and growth:  
842 evidence from competition with its cytosolic domain. *Plant Cell* **14**: 387-406.
- 843 **Geiger, D., Becker, D., Vosloh, D., Gambale, F., Palme, K., Rehers, M., Anschuetz, U.,**  
844 **Dreyer, I., Kudla, J., and Hedrich, R.** (2009). Heteromeric AtKC1-AKT1 channels in  
845 Arabidopsis roots facilitate growth under K<sup>+</sup>-limiting conditions. *J. Biol. Chem.* **284**: 21288–  
846 21295.
- 847 **Gray, A., Liu, L., and Facette, M.** (2020). Flanking Support: How subsidiary cells contribute to  
848 stomatal form and function. *Front. Plant Sci.* **11**: 1–12.
- 849 **Grefen, C., Karnik, R., Larson, E., Lefoulon, C., Wang, Y., Waghmare, S., Zhang, B., Hills, A.,**  
850 **and Blatt, M.R.** (2015). A vesicle-trafficking protein commandeers Kv channel voltage  
851 sensors for voltage-dependent secretion. *Nat. Plants* **1**: 15108.
- 852 **Hajdukiewicz, P., Svab, Z., and Maliga, P.** (1994). The small, versatile pPZP family of  
853 *Agrobacterium* binary vectors for plant transformation. *Plant Mol. Biol.* **25**, 989-994.
- 854 **Hedrich, R.** (2012). Ion channels in plants. *Physiol. Rev.* **92**: 1777-1811.
- 855 **Higaki, T., Hashimoto-Sugimoto, M., Akita, K., Iba, K., and Hasezawa, S.** (2014). Dynamics  
856 and environmental responses of PATROL1 in Arabidopsis subsidiary cells. *Plant Cell*  
857 *Physiol.* **55**: 773-780.
- 858 **Honsbein, A., Sokolovski, S., Grefen, C., Campanoni, P., Pratelli, R., Paneque, M., Chen, Z.,**  
859 **Johansson, I., and Blatt, M.R.** (2009). A tripartite SNARE-K<sup>+</sup> channel complex mediates in  
860 channel-dependent K<sup>+</sup> nutrition in Arabidopsis. *Plant Cell* **21** : 2859-2877.
- 861 **Hosy, E., Vavasseur, A., Mouline, K., Dreyer, I., Gaymard, F., Porée, F., Boucherez, J.,**  
862 **Lebaudy, A., Bouchez, D., Véry, A.-A., Simonneau, T., Thibaud, J.B., and Sentenac, H.**  
863 (2003). The Arabidopsis outward K<sup>+</sup> channel GORK is involved in regulation of stomatal  
864 movements and plant transpiration. *Proc. Natl. Acad. Sci. U S A* **100**: 5549-5554.
- 865 **Humble, G.D. and Raschke, K.** (1971). Stomatal opening quantitatively related to potassium  
866 transport: evidence from electron probe analysis. *Plant Physiol.* **48**: 447–453.
- 867 **Jakoby, M.J., Falkenhan, D., Mader, M.T., Brininstool, G., Wischnitzki, E., Platz, N., Hudson,**  
868 **A., Hulskamp, M., Larkin, J., and Schnittger, A.** (2008). Transcriptional profiling of mature  
869 Arabidopsis trichomes reveals that NOECK encodes the MIXTA-like transcriptional regulator  
870 MYB106. *Plant Physiol.* **148**: 1583-1602.

- 871 **Jammes, F., Leonhardt, N., Tran, D., Bousserouel, H., Véry, A.-A., Renou, J.-P., Vavasseur,**  
872 **A., Kwak, J.M., Sentenac, H., Bouteau, F., and Leung, J.** (2014). Acetylated 1,3-  
873 diaminopropane antagonizes abscisic acid-mediated stomatal closing in Arabidopsis. *Plant J.*  
874 **79:** 322-333.
- 875 **Jeanguenin, L., Alcon, C., Duby, G., Boeglin, M., Chérel, I., Gaillard, I., Zimmermann, S.,**  
876 **Sentenac, H., and Véry, A.-A.** (2011). AtKC1 is a general modulator of Arabidopsis inward  
877 Shaker channel activity. *Plant J.* **67:** 570-582.
- 878 **Jegla, T., Busey, G., and Assmann, S.M.** (2018). Evolution and structural characteristics of plant  
879 voltage-gated K<sup>+</sup> Channels. *Plant Cell* **30:** 2898-2909.
- 880 **Jezek, M., and Blatt, M.R.** (2017). The membrane transport system of the guard cell and its  
881 integration for stomatal dynamics. *Plant Physiol.* **174:** 487-519.
- 882 **Jezek, M., Hills, A., Blatt, M.R., and Lew, V.L.** (2019). A constraint-relaxation-recovery  
883 mechanism for stomatal dynamics. *Plant Cell Environ.* **42,** 2399-2410.
- 884 **Jin, X., Wang, R.S., Zhu, M., Jeon, B.W., Albert, R., Chen, S., and Assmann, S.M.** (2013).  
885 Abscisic acid-responsive guard cell metabolomes of Arabidopsis wild-type and *gpa1* G-  
886 protein mutants. *Plant Cell* **25:** 4789-4811.
- 887 **Kim, T.H., Bohmer, M., Hu, H., Nishimura, N., and Schroeder, J.I.** (2010). Guard cell signal  
888 transduction network: advances in understanding abscisic acid, CO<sub>2</sub>, and Ca<sup>2+</sup> signaling.  
889 *Annu. Rev. Plant Biol.* **61:** 561-591.
- 890 **Kufner, I., and Koch, W.** (2008). Stress regulated members of the plant organic cation transporter  
891 family are localized to the vacuolar membrane. *BMC Res. Notes* **1:** 43.
- 892 **Lacombe, B., Pilot, G., Michard, E., Gaymard, F., Sentenac, H., and Thibaud, J.B.** (2000). A  
893 shaker-like K<sup>+</sup> channel with weak rectification is expressed in both source and sink phloem  
894 tissues of Arabidopsis. *Plant Cell* **12:** 837-851.
- 895 **Lagarde, D., Basset, M., Lepetit, M., Conejero, G., Gaymard, F., Astruc, S., and Grignon, C.**  
896 (1996). Tissue-specific expression of Arabidopsis AKT1 gene is consistent with a role in K<sup>+</sup>  
897 nutrition. *Plant J.* **9:** 195-203.
- 898 **Lebaudy, A., Vavasseur, A., Hosy, E., Dreyer, I., Leonhardt, N., Thibaud, J.B., Véry, A.-A.,**  
899 **Simonneau, T., and Sentenac, H.** (2008). Plant adaptation to fluctuating environment and  
900 biomass production are strongly dependent on guard cell potassium channels. *Proc. Natl.*  
901 *Acad. Sci. U S A* **105:** 5271-5276.
- 902 **Lebaudy, A., Pascaud, F., Véry, A.-A., Alcon, C., Dreyer, I., Thibaud, J.-B., Lacombe, B.**  
903 (2010). Preferential KAT1-KAT2 heteromerization determines inward K<sup>+</sup> current properties in  
904 Arabidopsis guard cells. *J. Biol. Chem.* **285:** 6265-6274.

- 905 **Leonhardt, N., Kwak, J.M., Robert, N., Waner, D., Leonhardt, G., and Schroeder, J.I.** (2004).  
906 Microarray expression analyses of Arabidopsis guard cells and isolation of a recessive  
907 abscisic acid hypersensitive protein phosphatase 2C mutant. *Plant Cell* **16**: 596-615.
- 908 **Lieckfeldt, E., Simon-Rosin, U., Kose, F., Zoeller, D., Schliep, M., and Fisahn, J.** (2008). Gene  
909 expression profiling of single epidermal, basal and trichome cells of Arabidopsis thaliana. *J.*  
910 *Plant Physiol.* **165**: 1530-1544.
- 911 **Long, Y., Cheddadi, I., Mosca, G., Mirabet, V., Dumond, M., Kiss, A., Traas, J., Godin, C., and**  
912 **Boudaoud, A.** (2020). Cellular heterogeneity in pressure and growth emerges from tissue  
913 topology and geometry. *Curr. Biol.* **30**: 1504-1516.e8.
- 914 **MacRobbie, E.A.C.** (1980). Osmotic measurements on stomatal cells of *Commelina communis* L.  
915 *J. Membr. Biol.* **53**: 189-198.
- 916 **Malgat, R., Faure, F., and Boudaoud, A.** (2016). A mechanical model to interpret cell-scale  
917 indentation experiments on plant tissues in terms of cell wall elasticity and turgor pressure.  
918 *Front. Plant Sci.* **7**: 1351.
- 919 **Merlot, S., Leonhardt, N., Fenzi, F., Valon, C., Costa, M., Piette, L., Vavasseur, A., Genty, B.,**  
920 **Boivin, K., Muller, A., Giraudat, J., and Leung, J.** (2007). Constitutive activation of a  
921 plasma membrane H<sup>+</sup>-ATPase prevents abscisic acid-mediated stomatal closure. *EMBO J.*  
922 **26**: 3216-3226.
- 923 **Michard, E., Dreyer, I., Lacombe, B., Sentenac, H., and Thibaud, J.B.** (2005a). Inward  
924 rectification of the AKT2 channel abolished by voltage-dependent phosphorylation. *Plant J.*  
925 **44**: 783-797.
- 926 **Michard, E., Lacombe, B., Porée, F., Mueller-Roeber, B., Sentenac, H., Thibaud, J.B., and**  
927 **Dreyer, I.** (2005b). A unique voltage sensor sensitizes the potassium channel AKT2 to  
928 phosphoregulation. *J. Gen. Physiol.* **126**: 605-617.
- 929 **Misra, B.B., Acharya, B.R., Granot, D., Assmann, S.M., and Chen, S.** (2015). The guard cell  
930 metabolome: functions in stomatal movement and global food security. *Front. Plant Sci.* **6**:  
931 334.
- 932 **Mott, K.A. and Buckley, T.N.** (2000). Patchy stomatal conductance: Emergent collective  
933 behaviour of stomata. *Trends Plant Sci.* **5**: 258–262.
- 934 **Mustroph, A., Zanetti, M.E., Jang, C.J., Holtan, H.E., Repetti, P.P., Galbraith, D.W., Girke, T.,**  
935 **and Bailey-Serres, J.** (2009). Profiling transcriptomes of discrete cell populations resolves  
936 altered cellular priorities during hypoxia in Arabidopsis. *Proc. Natl. Acad. Sci. U S A* **106**:  
937 18843-18848.
- 938 **Nakagawa, T., Kurose, T., Hino, T., Tanaka, K., Kawamukai, M., Niwa, Y., Toyooka, K.,**  
939 **Matsuoka, K., Jinbo, T., and Kimura, T.** (2007). Development of series of gateway binary

- 940 vectors, pGWBs, for realizing efficient construction of fusion genes for plant transformation.  
941 J. Biosci. Bioeng. **104**: 34-41.
- 942 **Nakamura, R.L., McKendree, W.L., Jr., Hirsch, R.E., Sedbrook, J.C., Gaber, R.F., and**  
943 **Sussman, M.R.** (1995). Expression of an Arabidopsis potassium channel gene in guard  
944 cells. Plant Physiol. **109**: 371-374.
- 945 **Nguyen, T.H., Huang, S., Meynard, D., Chaine, C., Michel, R., Roelfsema, M.R.G.,**  
946 **Guideroni, E., Sentenac, H., and Véry, A.-A.** (2017). A dual role for the OsK5.2 ion  
947 channel in stomatal movements and K<sup>+</sup> loading into Xylem Sap. Plant Physiol. **174**: 2409–  
948 2418.
- 949 **Nieves-Cordones, M., Caballero, F., Martinez, V., and Rubio, F.** (2012). Disruption of the  
950 *Arabidopsis thaliana* inward-rectifier K<sup>+</sup> channel AKT1 improves plant responses to water  
951 stress. Plant Cell Physiol. **53**: 423-432.
- 952 **Nieves-Cordones, M., Chavanieu, A., Jeanguenin, L., Alcon, C., Szponarski, W., Estaran, S.,**  
953 **Chérel, I., Zimmermann, S., Sentenac, H., and Gaillard, I.** (2014). Distinct amino acids in  
954 the C-linker domain of the Arabidopsis K<sup>+</sup> channel KAT2 determine its subcellular localization  
955 and activity at the plasma membrane. Plant Physiol. **164**: 1415-1429.
- 956 **Olszak, B., Malinovsky, F.G., Brodersen, P., Grell, M., Giese, H., Petersen, M., and Mundy, J.**  
957 (2006). A putative flavin-containing mono-oxygenase as a marker for certain defense and cell  
958 death pathways. Plant Sci. **170**: 614-623.
- 959 **Obrdlik, P. et al.** (2004). K<sup>+</sup> channel interactions detected by a genetic system optimized for  
960 systematic studies of membrane protein interactions. Proc. Natl. Acad. Sci. U. S. A. **101**:  
961 12242–12247.
- 962 **Palevitz, B.A., and Hepler, P.K.** (1985). Changes in dye coupling of stomatal cells of *Allium* and  
963 *Commelina* demonstrated by microinjection of Lucifer yellow. Planta **164**: 473-479.
- 964 **Pandey, S., Zhang, W., and Assmann, S.M.** (2007). Roles of ion channels and transporters in  
965 guard cell signal transduction. FEBS Lett. **581**: 2325-2336.
- 966 **Pighin, J.A., Zheng, H., Balakshin, L.J., Goodman, I.P., Western, T.L., Jetter, R., Kunst, L.,**  
967 **and Samuels, A.L.** (2004). Plant cuticular lipid export requires an ABC transporter. Science  
968 **306**: 702-704.
- 969 **Pilot, G., Gaymard, F., Mouline, K., Chérel, I., and Sentenac, H.** (2003). Regulated expression  
970 of Arabidopsis shaker K<sup>+</sup> channel genes involved in K<sup>+</sup> uptake and distribution in the plant.  
971 Plant Mol. Biol. **51**: 773-787.
- 972 **Pilot, G., Lacombe, B., Gaymard, F., Chérel, I., Boucherez, J., Thibaud, J.B., and Sentenac,**  
973 **H.** (2001). Guard cell inward K<sup>+</sup> channel activity in arabidopsis involves expression of the twin  
974 channel subunits KAT1 and KAT2. J. Biol. Chem. **276**: 3215-3221.

- 975 **Reintanz, B., Szyroki, A., Ivashikina, N., Ache, P., Godde, M., Becker, D., Palme, K., and**  
976 **Hedrich, R.** (2002). AtKC1, a silent Arabidopsis potassium channel alpha -subunit modulates  
977 root hair K<sup>+</sup> influx. Proc. Natl. Acad. Sci. U S A **99**: 4079-4084.
- 978 **Roelfsema, M.R.G. and Prins, H.B.A.** (1997). Ion channels in guard cells of *Arabidopsis thaliana*  
979 (L.) Heynh. Planta **202**: 18–27.
- 980 **Rohaim, A., Gong, L.D., Li, J., Rui, H., Blachowicz, L., and Roux, B.** (2020). Open and closed  
981 structures of a barium-blocked potassium channel. J. Mol. Biol. **432**: 4783–4798.
- 982 **Schliep, M., Ebert, B., Simon-Rosin, U., Zoeller, D., and Fisahn, J.** (2010). Quantitative  
983 expression analysis of selected transcription factors in pavement, basal and trichome cells of  
984 mature leaves from Arabidopsis thaliana. Protoplasma **241**: 29-36.
- 985 **Schroeder, J.I., Raschke, K., and Neher, E.** (1987). Voltage dependence of K<sup>+</sup> channels in  
986 guard-cell protoplasts. Proc. Natl. Acad. Sci. U S A **84**: 4108-4112.
- 987 **Spalding, E.P., Hirsch, R.E., Lewis, D.R., Qi, Z., Sussman, M.R., and Bryan D., L.** (1999).  
988 Potassium Uptake Supporting Plant Growth in the Absence of AKT1 Channel Activity. J.  
989 Gen. Physiol. **113**: 909–918.
- 990 **Su, Y.H., North, H., Grignon, C., Thibaud, J.B., Sentenac, H., and Véry, A.A.** (2005).  
991 Regulation by external K<sup>+</sup> in a maize inward shaker channel targets transport activity in the  
992 high concentration range. Plant Cell **17**: 1532–1548.
- 993 **Szymanski, D.B., Jilk, R.A., Pollock, S.M., and Marks, M.D.** (1998). Control of GL2 expression  
994 in Arabidopsis leaves and trichomes. Development **125**: 1161-1171.
- 995 **Szyroki, A., Ivashikina, N., Dietrich, P., Roelfsema, M.R.G., Ache, P., Reintanz, B., Deeken,**  
996 **R., Godde, M., Felle, H., Steinmeyer, R., Palme, K., and Hedrich, R.** (2001). KAT1 is not  
997 essential for stomatal opening. Proc. Natl. Acad. Sci. U. S. A. **98**: 2917–2921.
- 998 **Talbott, L.D. and Zeiger, E.** (1996). Central roles for potassium and sucrose in guard-cell  
999 osmoregulation. Plant Physiol. **111**: 1051–1057.
- 000 **Telfer, A., Bollman, K.M., and Poethig, R.S.** (1997). Phase change and the regulation of  
001 trichome distribution in *Arabidopsis thaliana*. Development **124**: 645-654.
- 002 **Tominaga, M., Kinoshita, T., and Shimazaki, K.-I.** (2001). Guard-cell chloroplasts provide ATP  
003 required for H<sup>+</sup> pumping in the plasma membrane and stomatal opening. Plant Cell Physiol.  
004 **42**: 795-802.
- 005 **Urbach, S., Chérel, I., Sentenac, H., and Gaymard, F.** (2000). Biochemical characterization of  
006 the Arabidopsis K<sup>+</sup> channels KAT1 and AKT1 expressed or co-expressed in insect cells.  
007 Plant J. **23**: 527-538.
- 008 **Verger, S., Long, Y., Boudaoud, A., and Hamant, O.** (2018). A tension-adhesion feedback loop  
009 in plant epidermis. Elife **7**: 1–25.



- 010 **Véry, A.-A. and Sentenac, H.** (2002). Cation channels in the Arabidopsis plasma membrane.  
011 Trends Plant Sci. **7**: 168–175.
- 012 **Véry, A.-A., and Sentenac, H.** (2003). Molecular mechanisms and regulation of K<sup>+</sup> transport in  
013 higher plants. Annu. Rev. Plant Biol. **54**: 575-603.
- 014 **Véry, A.-A., Nieves-Cordones, M., Daly, M., Khan, I., Fizames, C., and Sentenac, H.** (2014).  
015 Molecular biology of K<sup>+</sup> transport across the plant cell membrane: what do we learn from  
016 comparison between plant species? J. Plant Physiol. **171**: 748-769.
- 017 **Wang, R.S., Pandey, S., Li, S., Gookin, T.E., Zhao, Z., Albert, R., and Assmann, S.M.** (2011).  
018 Common and unique elements of the ABA-regulated transcriptome of Arabidopsis guard  
019 cells. BMC Genomics **12**: 216.
- 020 **Wang, X.P., Chen, L.M., Liu, W.X., Shen, L.K., Wang, F.L., Zhou, Y., Zhang, Z., Wu, W.H., and**  
021 **Wang, Y.** (2016). AtKC1 and CIPK23 Synergistically Modulate AKT1-Mediated Low-  
022 Potassium Stress Responses in Arabidopsis. Plant Physiol. **170**: 2264-2277.
- 023 **Wegner, L.H., Boer, A.H. De, and Raschke, K.** (1994). Properties of the K<sup>+</sup> inward rectifier in the  
024 plasma membrane of xylem parenchyma cells from barley roots: effects of TEA<sup>+</sup>, Ca<sup>2+</sup>, Ba<sup>2+</sup>  
025 and La<sup>3+</sup>. J. Membr. Biol. **142**: 363–379.
- 026 **Wille, A.C., and Lucas, W.J.** (1984). Ultrastructural and histochemical studies on guard cells.  
027 Planta **160**: 129-142.
- 028 **Zhang, B., Karnik, R., Wang, Y., Wallmeroth, N., Blatt, M.R., and Grefen, C.** (2015). The  
029 Arabidopsis R-SNARE VAMP721 interacts with KAT1 and KC1 K<sup>+</sup> channels to moderate K<sup>+</sup>  
030 current at the plasma membrane. Plant Cell **27**: 1697-1717.
- 031 **Zhao, Z., Zhang, W., Stanley, B.A., and Assmann, S.M.** (2008). Functional proteomics of  
032 *Arabidopsis thaliana* guard cells uncovers new stomatal signaling pathways. Plant Cell **20**:  
033 3210-3226.
- 034 **Zhou, L.H., Liu, S.B., Wang, P.F., Lu, T.J., Xu, F., Genin, G.M., and Pickard, B.G.** (2017). The  
035 Arabidopsis trichome is an active mechanosensory switch. Plant Cell Environ. **40**: 611-621.
- 036 **Zhu, M., and Assmann, S.M.** (2017). Metabolic signatures in response to abscisic acid (ABA)  
037 treatment in *Brassica napus* Guard cells revealed by metabolomics. Sci. Rep. **7**: 12875  
038  
039

## Parsed Citations

Bauer, H., Ache, P., Lautner, S., Fromm, J., Hartung, W., Al-Rasheid, K.A., Sonnewald, S., Sonnewald, U., Kneitz, S., Lachmann, N., Mendel, R.R., Bittner, F., Hetherington, A.M., and Hedrich, R. (2013). The stomatal response to reduced relative humidity requires guard cell-autonomous ABA synthesis. *Curr. Biol.* 23: 53-57.

Google Scholar: [Author Only](#) [Title Only](#) [Author and Title](#)

Beauzamy, L., Derr, J., and Boudaoud, A. (2015). Quantifying hydrostatic pressure in plant cells by using indentation with an atomic force microscope. *Biophys. J.* 108: 2448-2456.

Google Scholar: [Author Only](#) [Title Only](#) [Author and Title](#)

Blatt, M.R. (2000). Cellular signaling and volume control in stomatal movements in plants. *Annu. Rev. Cell. Dev. Biol.* 16: 221-241.

Google Scholar: [Author Only](#) [Title Only](#) [Author and Title](#)

Britto, D.T., Coskun, D., and Kronzucker, H.J. (2021). Potassium physiology from Archaean to Holocene: A higher-plant perspective. *J. Plant Physiol.* 262: 153432.

Google Scholar: [Author Only](#) [Title Only](#) [Author and Title](#)

Clough, S.J., and Bent, A.F. (1998). Floral dip: a simplified method for *Agrobacterium*-mediated transformation of *Arabidopsis thaliana*. *Plant J.* 16: 735-743.

Google Scholar: [Author Only](#) [Title Only](#) [Author and Title](#)

Cuellar, T., Pascaud, F., Verdeil, J.L., Torregrosa, L., Adam-Blondon, A.F., Thibaud, J.B., Sentenac, H., and Gaillard, I. (2010). A grapevine Shaker inward K<sup>+</sup> channel activated by the calcineurin B-like calcium sensor 1-protein kinase CIPK23 network is expressed in grape berries under drought stress conditions. *Plant J.* 61: 58-69.

Google Scholar: [Author Only](#) [Title Only](#) [Author and Title](#)

Czechowski, T., Stitt, M., Altmann, T., Udvardi, M.K., and Scheible, W.R. (2005). Genome-wide identification and testing of superior reference genes for transcript normalization in *Arabidopsis*. *Plant Physiol.* 139: 5-17.

Google Scholar: [Author Only](#) [Title Only](#) [Author and Title](#)

Daram, P., Urbach, S., Gaymard, F., Sentenac, H., and Chérel, I. (1997). Tetramerization of the AKT1 plant potassium channel involves its C-terminal cytoplasmic domain. *EMBO J.* 16: 3455-3463.

Google Scholar: [Author Only](#) [Title Only](#) [Author and Title](#)

Duby, G., Hosal, E., Fizames, C., Alcon, C., Costa, A., Sentenac, H., and Thibaud, J.B. (2008). AtKC1, a conditionally targeted Shaker-type subunit, regulates the activity of plant K<sup>+</sup> channels. *Plant J.* 53: 115-123.

Google Scholar: [Author Only](#) [Title Only](#) [Author and Title](#)

Franks, P.J., Cowan, I.R., and Farquhar, G.D. (1998). A study of stomatal mechanics using the cell pressure probe. *Plant Cell Environ.* 21: 94-100.

Google Scholar: [Author Only](#) [Title Only](#) [Author and Title](#)

Franks, P.J., Buckley, T.N., Shope, J.C., and Mott, K.A. (2001). Guard cell volume and pressure measured concurrently by confocal microscopy and the cell pressure probe. *Plant Physiol.* 125: 1577-1584.

Google Scholar: [Author Only](#) [Title Only](#) [Author and Title](#)

Franks, P.J., Cowan, I.R., Tyerman, S.D., Cleary, A.L., Lloyd, J., and Farquhar, G.D. (1995). Guard-cell pressure aperture characteristics measured with the pressure probe. *Plant Cell Environ.* 18: 795-800.

Google Scholar: [Author Only](#) [Title Only](#) [Author and Title](#)

Geelen, D., Leyman, B., Batoko, H., Di Sansebastiano, G.P., Moore, I., and Blatt, M.R. (2002). The abscisic acid-related SNARE homolog NtSyr1 contributes to secretion and growth: evidence from competition with its cytosolic domain. *Plant Cell* 14: 387-406.

Google Scholar: [Author Only](#) [Title Only](#) [Author and Title](#)

Geiger, D., Becker, D., Vosloh, D., Gambale, F., Palme, K., Rehers, M., Anschuetz, U., Dreyer, I., Kudla, J., and Hedrich, R. (2009). Heteromeric AtKC1-AKT1 channels in *Arabidopsis* roots facilitate growth under K<sup>+</sup>-limiting conditions. *J. Biol. Chem.* 284: 21288-21295.

Google Scholar: [Author Only](#) [Title Only](#) [Author and Title](#)

Gray, A., Liu, L., and Facette, M. (2020). Flanking Support: How subsidiary cells contribute to stomatal form and function. *Front. Plant Sci.* 11: 1-12.

Google Scholar: [Author Only](#) [Title Only](#) [Author and Title](#)

Grefen, C., Karnik, R., Larson, E., Lefoulon, C., Wang, Y., Waghmare, S., Zhang, B., Hills, A., and Blatt, M.R. (2015). A vesicle-trafficking protein commandeers Kv channel voltage sensors for voltage-dependent secretion. *Nat. Plants* 1: 15108.

Google Scholar: [Author Only](#) [Title Only](#) [Author and Title](#)

Hajdukiewicz, P., Svab, Z., and Maliga, P. (1994). The small, versatile pPZP family of *Agrobacterium* binary vectors for plant transformation. *Plant Mol. Biol.* 25, 989-994.

Google Scholar: [Author Only](#) [Title Only](#) [Author and Title](#)

**Hedrich, R. (2012).** Ion channels in plants. *Physiol. Rev.* 92: 1777-1811.

Google Scholar: [Author Only](#) [Title Only](#) [Author and Title](#)

**Higaki, T., Hashimoto-Sugimoto, M., Akita, K., Iba, K., and Hasezawa, S. (2014).** Dynamics and environmental responses of PATROL1 in *Arabidopsis* subsidiary cells. *Plant Cell Physiol.* 55: 773-780.

Google Scholar: [Author Only](#) [Title Only](#) [Author and Title](#)

**Honsbein, A., Sokolovski, S., Grefen, C., Campanoni, P., Pratelli, R., Paneque, M., Chen, Z., Johansson, I., and Blatt, M.R. (2009).** A tripartite SNARE-K<sup>+</sup> channel complex mediates in channel-dependent K<sup>+</sup> nutrition in *Arabidopsis*. *Plant Cell* 21 : 2859-2877.

Google Scholar: [Author Only](#) [Title Only](#) [Author and Title](#)

**Hosy, E., Vavasseur, A., Mouline, K., Dreyer, I., Gaymard, F., Porée, F., Boucherez, J., Lebaudy, A., Bouchez, D., Véry, A-A, Simonneau, T., Thibaud, J.B., and Sentenac, H. (2003).** The *Arabidopsis* outward K<sup>+</sup> channel GORK is involved in regulation of stomatal movements and plant transpiration. *Proc. Natl. Acad. Sci. U S A* 100: 5549-5554.

Google Scholar: [Author Only](#) [Title Only](#) [Author and Title](#)

**Humble, G.D. and Raschke, K. (1971).** Stomatal opening quantitatively related to potassium transport: evidence from electron probe analysis. *Plant Physiol.* 48: 447-453.

Google Scholar: [Author Only](#) [Title Only](#) [Author and Title](#)

**Jakoby, M.J., Falkenhan, D., Mader, M.T., Brininstool, G., Wischnitzki, E., Platz, N., Hudson, A., Hulskamp, M., Larkin, J., and Schnittger, A. (2008).** Transcriptional profiling of mature *Arabidopsis* trichomes reveals that NOECK encodes the MIXTA-like transcriptional regulator MYB106. *Plant Physiol.* 148: 1583-1602.

Google Scholar: [Author Only](#) [Title Only](#) [Author and Title](#)

**Jammes, F., Leonhardt, N., Tran, D., Bousserouel, H., Véry, A-A, Renou, J.-P., Vavasseur, A., Kwak, J.M., Sentenac, H., Bouteau, F., and Leung, J. (2014).** Acetylated 1,3-diaminopropane antagonizes abscisic acid-mediated stomatal closing in *Arabidopsis*. *Plant J.* 79: 322-333.

Google Scholar: [Author Only](#) [Title Only](#) [Author and Title](#)

**Jeanguenin, L., Alcon, C., Duby, G., Boeglin, M., Chérel, I., Gaillard, I., Zimmermann, S., Sentenac, H., and Véry, A-A (2011).** AtKC1 is a general modulator of *Arabidopsis* inward Shaker channel activity. *Plant J.* 67: 570-582.

Google Scholar: [Author Only](#) [Title Only](#) [Author and Title](#)

**Jegla, T., Busey, G., and Assmann, S.M. (2018).** Evolution and structural characteristics of plant voltage-gated K<sup>+</sup> Channels. *Plant Cell* 30: 2898-2909.

Google Scholar: [Author Only](#) [Title Only](#) [Author and Title](#)

**Jezeq, M., and Blatt, M.R. (2017).** The membrane transport system of the guard cell and its integration for stomatal dynamics. *Plant Physiol.* 174: 487-519.

Google Scholar: [Author Only](#) [Title Only](#) [Author and Title](#)

**Jezeq, M., Hills, A., Blatt, M.R., and Lew, V.L. (2019).** A constraint-relaxation-recovery mechanism for stomatal dynamics. *Plant Cell Environ.* 42, 2399-2410.

Google Scholar: [Author Only](#) [Title Only](#) [Author and Title](#)

**Jin, X., Wang, R.S., Zhu, M., Jeon, B.W., Albert, R., Chen, S., and Assmann, S.M. (2013).** Abscisic acid-responsive guard cell metabolomes of *Arabidopsis* wild-type and *gpa1* G-protein mutants. *Plant Cell* 25: 4789-4811.

Google Scholar: [Author Only](#) [Title Only](#) [Author and Title](#)

**Kim, T.H., Bohmer, M., Hu, H., Nishimura, N., and Schroeder, J.I. (2010).** Guard cell signal transduction network: advances in understanding abscisic acid, CO<sub>2</sub>, and Ca<sup>2+</sup> signaling. *Annu. Rev. Plant Biol.* 61: 561-591.

Google Scholar: [Author Only](#) [Title Only](#) [Author and Title](#)

**Kufner, I., and Koch, W. (2008).** Stress regulated members of the plant organic cation transporter family are localized to the vacuolar membrane. *BMC Res. Notes* 1: 43.

Google Scholar: [Author Only](#) [Title Only](#) [Author and Title](#)

**Lacombe, B., Pilot, G., Michard, E., Gaymard, F., Sentenac, H., and Thibaud, J.B. (2000).** A shaker-like K<sup>+</sup> channel with weak rectification is expressed in both source and sink phloem tissues of *Arabidopsis*. *Plant Cell* 12: 837-851.

Google Scholar: [Author Only](#) [Title Only](#) [Author and Title](#)

**Lagarde, D., Basset, M., Lepetit, M., Conejero, G., Gaymard, F., Astruc, S., and Grignon, C. (1996).** Tissue-specific expression of *Arabidopsis* AKT1 gene is consistent with a role in K<sup>+</sup> nutrition. *Plant J.* 9: 195-203.

Google Scholar: [Author Only](#) [Title Only](#) [Author and Title](#)

**Lebaudy, A., Vavasseur, A., Hosy, E., Dreyer, I., Leonhardt, N., Thibaud, J.B., Véry, A-A, Simonneau, T., and Sentenac, H. (2008).** Plant adaptation to fluctuating environment and biomass production are strongly dependent on guard cell potassium channels. *Proc. Natl. Acad. Sci. U S A* 105: 5271-5276.

Google Scholar: [Author Only](#) [Title Only](#) [Author and Title](#)

Lebaudy, A., Pascaud, F., Véry, A-A, Alcon, C., Dreyer, I., Thibaud, J.-B., Lacombe, B. (2010). Preferential KAT1-KAT2 heteromerization determines inward K<sup>+</sup> current properties in *Arabidopsis* guard cells. *J. Biol. Chem.* 285: 6265-6274.

Google Scholar: [Author Only](#) [Title Only](#) [Author and Title](#)

Leonhardt, N., Kwak, J.M., Robert, N., Waner, D., Leonhardt, G., and Schroeder, J.I. (2004). Microarray expression analyses of *Arabidopsis* guard cells and isolation of a recessive abscisic acid hypersensitive protein phosphatase 2C mutant. *Plant Cell* 16: 596-615.

Google Scholar: [Author Only](#) [Title Only](#) [Author and Title](#)

Lieckfeldt, E., Simon-Rosin, U., Kose, F., Zoeller, D., Schliep, M., and Fisahn, J. (2008). Gene expression profiling of single epidermal, basal and trichome cells of *Arabidopsis thaliana*. *J. Plant Physiol.* 165: 1530-1544.

Google Scholar: [Author Only](#) [Title Only](#) [Author and Title](#)

Long, Y., Cheddadi, I., Mosca, G., Mirabet, V., Dumond, M., Kiss, A., Traas, J., Godin, C., and Boudaoud, A. (2020). Cellular heterogeneity in pressure and growth emerges from tissue topology and geometry. *Curr. Biol.* 30: 1504-1516.e8.

Google Scholar: [Author Only](#) [Title Only](#) [Author and Title](#)

MacRobbie, E.A.C. (1980). Osmotic measurements on stomatal cells of *Commelina communis* L. *J. Membr. Biol.* 53: 189-198.

Google Scholar: [Author Only](#) [Title Only](#) [Author and Title](#)

Malgat, R., Faure, F., and Boudaoud, A. (2016). A mechanical model to interpret cell-scale indentation experiments on plant tissues in terms of cell wall elasticity and turgor pressure. *Front. Plant Sci.* 7: 1351.

Google Scholar: [Author Only](#) [Title Only](#) [Author and Title](#)

Merlot, S., Leonhardt, N., Fenzi, F., Valon, C., Costa, M., Piette, L., Vavasseur, A., Genty, B., Boivin, K., Muller, A., Giraudat, J., and Leung, J. (2007). Constitutive activation of a plasma membrane H<sup>+</sup>-ATPase prevents abscisic acid-mediated stomatal closure. *EMBO J.* 26: 3216-3226.

Google Scholar: [Author Only](#) [Title Only](#) [Author and Title](#)

Michard, E., Dreyer, I., Lacombe, B., Sentenac, H., and Thibaud, J.B. (2005a). Inward rectification of the AKT2 channel abolished by voltage-dependent phosphorylation. *Plant J.* 44: 783-797.

Google Scholar: [Author Only](#) [Title Only](#) [Author and Title](#)

Michard, E., Lacombe, B., Porée, F., Mueller-Roeber, B., Sentenac, H., Thibaud, J.B., and Dreyer, I. (2005b). A unique voltage sensor sensitizes the potassium channel AKT2 to phosphoregulation. *J. Gen. Physiol.* 126: 605-617.

Google Scholar: [Author Only](#) [Title Only](#) [Author and Title](#)

Misra, B.B., Acharya, B.R., Granot, D., Assmann, S.M., and Chen, S. (2015). The guard cell metabolome: functions in stomatal movement and global food security. *Front. Plant Sci.* 6: 334.

Google Scholar: [Author Only](#) [Title Only](#) [Author and Title](#)

Mott, K.A. and Buckley, T.N. (2000). Patchy stomatal conductance: Emergent collective behaviour of stomata. *Trends Plant Sci.* 5: 258-262.

Google Scholar: [Author Only](#) [Title Only](#) [Author and Title](#)

Mustroph, A., Zanetti, M.E., Jang, C.J., Holtan, H.E., Repetti, P.P., Galbraith, D.W., Girke, T., and Bailey-Serres, J. (2009). Profiling transcriptomes of discrete cell populations resolves altered cellular priorities during hypoxia in *Arabidopsis*. *Proc. Natl. Acad. Sci. U S A* 106: 18843-18848.

Google Scholar: [Author Only](#) [Title Only](#) [Author and Title](#)

Nakagawa, T., Kurose, T., Hino, T., Tanaka, K., Kawamukai, M., Niwa, Y., Toyooka, K., Matsuoka, K., Jinbo, T., and Kimura, T. (2007). Development of series of gateway binary vectors, pGWBs, for realizing efficient construction of fusion genes for plant transformation. *J. Biosci. Bioeng.* 104: 34-41.

Google Scholar: [Author Only](#) [Title Only](#) [Author and Title](#)

Nakamura, R.L., McKendree, W.L., Jr., Hirsch, R.E., Sedbrook, J.C., Gaber, R.F., and Sussman, M.R. (1995). Expression of an *Arabidopsis* potassium channel gene in guard cells. *Plant Physiol.* 109: 371-374.

Google Scholar: [Author Only](#) [Title Only](#) [Author and Title](#)

Nguyen, T.H., Huang, S., Meynard, D., Chaine, C., Michel, R., Roelfsema, M.R.G., Guiderdoni, E., Sentenac, H., and Véry, A-A. (2017). A dual role for the OsK5.2 ion channel in stomatal movements and K<sup>+</sup> loading into Xylem Sap. *Plant Physiol.* 174: 2409-2418.

Google Scholar: [Author Only](#) [Title Only](#) [Author and Title](#)

Nieves-Cordones, M., Caballero, F., Martinez, V., and Rubio, F. (2012). Disruption of the *Arabidopsis thaliana* inward-rectifier K<sup>+</sup> channel AKT1 improves plant responses to water stress. *Plant Cell Physiol.* 53: 423-432.

Google Scholar: [Author Only](#) [Title Only](#) [Author and Title](#)

Nieves-Cordones, M., Chavanieu, A., Jeanguenin, L., Alcon, C., Szponarski, W., Estaran, S., Chérel, I., Zimmermann, S., Sentenac,

H., and Gaillard, I. (2014). Distinct amino acids in the C-linker domain of the Arabidopsis K<sup>+</sup> channel KAT2 determine its subcellular localization and activity at the plasma membrane. *Plant Physiol.* 164: 1415-1429.

Google Scholar: [Author Only](#) [Title Only](#) [Author and Title](#)

Olszak, B., Malinovsky, F.G., Brodersen, P., Grell, M., Giese, H., Petersen, M., and Mundy, J. (2006). A putative flavin-containing mono-oxygenase as a marker for certain defense and cell death pathways. *Plant Sci.* 170: 614-623.

Google Scholar: [Author Only](#) [Title Only](#) [Author and Title](#)

Obrdlik, P. et al. (2004). K<sup>+</sup> channel interactions detected by a genetic system optimized for systematic studies of membrane protein interactions. *Proc. Natl. Acad. Sci. U. S. A.* 101: 12242–12247.

Google Scholar: [Author Only](#) [Title Only](#) [Author and Title](#)

Palevitz, B.A., and Hepler, P.K. (1985). Changes in dye coupling of stomatal cells of *Allium* and *Commelina* demonstrated by microinjection of Lucifer yellow. *Planta* 164: 473-479.

Google Scholar: [Author Only](#) [Title Only](#) [Author and Title](#)

Pandey, S., Zhang, W., and Assmann, S.M. (2007). Roles of ion channels and transporters in guard cell signal transduction. *FEBS Lett.* 581: 2325-2336.

Google Scholar: [Author Only](#) [Title Only](#) [Author and Title](#)

Pighin, J.A., Zheng, H., Balakshin, L.J., Goodman, I.P., Western, T.L., Jetter, R., Kunst, L., and Samuels, A.L. (2004). Plant cuticular lipid export requires an ABC transporter. *Science* 306: 702-704.

Google Scholar: [Author Only](#) [Title Only](#) [Author and Title](#)

Pilot, G., Gaymard, F., Mouline, K., Chérel, I., and Sentenac, H. (2003). Regulated expression of Arabidopsis shaker K<sup>+</sup> channel genes involved in K<sup>+</sup> uptake and distribution in the plant. *Plant Mol. Biol.* 51: 773-787.

Google Scholar: [Author Only](#) [Title Only](#) [Author and Title](#)

Pilot, G., Lacombe, B., Gaymard, F., Chérel, I., Boucherez, J., Thibaud, J.B., and Sentenac, H. (2001). Guard cell inward K<sup>+</sup> channel activity in arabidopsis involves expression of the twin channel subunits KAT1 and KAT2. *J. Biol. Chem.* 276: 3215-3221.

Google Scholar: [Author Only](#) [Title Only](#) [Author and Title](#)

Reintanz, B., Szyroki, A., Ivashikina, N., Ache, P., Godde, M., Becker, D., Palme, K., and Hedrich, R. (2002). AtKC1, a silent Arabidopsis potassium channel alpha -subunit modulates root hair K<sup>+</sup> influx. *Proc. Natl. Acad. Sci. U S A* 99: 4079-4084.

Google Scholar: [Author Only](#) [Title Only](#) [Author and Title](#)

Roelfsema, M.R.G. and Prins, H.B.A (1997). Ion channels in guard cells of Arabidopsis thaliana (L.) Heynh. *Planta* 202: 18–27.

Google Scholar: [Author Only](#) [Title Only](#) [Author and Title](#)

Rohaim, A., Gong, L.D., Li, J., Rui, H., Blachowicz, L., and Roux, B. (2020). Open and closed structures of a barium-blocked potassium channel. *J. Mol. Biol.* 432: 4783–4798.

Google Scholar: [Author Only](#) [Title Only](#) [Author and Title](#)

Schliep, M., Ebert, B., Simon-Rosin, U., Zoeller, D., and Fisahn, J. (2010). Quantitative expression analysis of selected transcription factors in pavement, basal and trichome cells of mature leaves from Arabidopsis thaliana. *Protoplasma* 241: 29-36.

Google Scholar: [Author Only](#) [Title Only](#) [Author and Title](#)

Schroeder, J.I., Raschke, K., and Neher, E. (1987). Voltage dependence of K<sup>+</sup> channels in guard-cell protoplasts. *Proc. Natl. Acad. Sci. U S A* 84: 4108-4112.

Google Scholar: [Author Only](#) [Title Only](#) [Author and Title](#)

Spalding, E.P., Hirsch, R.E., Lewis, D.R., Qi, Z., Sussman, M.R., and Bryan D., L. (1999). Potassium Uptake Supporting Plant Growth in the Absence of AKT1 Channel Activity. *J. Gen. Physiol.* 113: 909–918.

Google Scholar: [Author Only](#) [Title Only](#) [Author and Title](#)

Su, Y.H., North, H., Grignon, C., Thibaud, J.B., Sentenac, H., and Véry, A.A. (2005). Regulation by external K<sup>+</sup> in a maize inward shaker channel targets transport activity in the high concentration range. *Plant Cell* 17: 1532–1548.

Google Scholar: [Author Only](#) [Title Only](#) [Author and Title](#)

Szymanski, D.B., Jilk, R.A., Pollock, S.M., and Marks, M.D. (1998). Control of GL2 expression in Arabidopsis leaves and trichomes. *Development* 125: 1161-1171.

Google Scholar: [Author Only](#) [Title Only](#) [Author and Title](#)

Szyroki, A., Ivashikina, N., Dietrich, P., Roelfsema, M.R.G., Ache, P., Reintanz, B., Deeken, R., Godde, M., Felle, H., Steinmeyer, R., Palme, K., and Hedrich, R. (2001). KAT1 is not essential for stomatal opening. *Proc. Natl. Acad. Sci. U. S. A.* 98: 2917–2921.

Google Scholar: [Author Only](#) [Title Only](#) [Author and Title](#)

Talbott, L.D. and Zeiger, E. (1996). Central roles for potassium and sucrose in guard-cell osmoregulation. *Plant Physiol.* 111: 1051–1057.

Google Scholar: [Author Only](#) [Title Only](#) [Author and Title](#)



- Telfer, A., Bollman, K.M., and Poethig, R.S. (1997). Phase change and the regulation of trichome distribution in *Arabidopsis thaliana*. *Development* 124: 645-654.  
Google Scholar: [Author Only](#) [Title Only](#) [Author and Title](#)
- Tominaga, M., Kinoshita, T., and Shimazaki, K.-I. (2001). Guard-cell chloroplasts provide ATP required for H<sup>+</sup> pumping in the plasma membrane and stomatal opening. *Plant Cell Physiol.* 42: 795-802.  
Google Scholar: [Author Only](#) [Title Only](#) [Author and Title](#)
- Urbach, S., Chérel, I., Sentenac, H., and Gaymard, F. (2000). Biochemical characterization of the *Arabidopsis* K<sup>+</sup> channels KAT1 and AKT1 expressed or co-expressed in insect cells. *Plant J.* 23: 527-538.  
Google Scholar: [Author Only](#) [Title Only](#) [Author and Title](#)
- Verger, S., Long, Y., Boudaoud, A., and Hamant, O. (2018). A tension-adhesion feedback loop in plant epidermis. *Elife* 7: 1–25.  
Google Scholar: [Author Only](#) [Title Only](#) [Author and Title](#)
- Véry, A.-A. and Sentenac, H. (2002). Cation channels in the *Arabidopsis* plasma membrane. *Trends Plant Sci.* 7: 168–175.  
Google Scholar: [Author Only](#) [Title Only](#) [Author and Title](#)
- Véry, A.-A., and Sentenac, H. (2003). Molecular mechanisms and regulation of K<sup>+</sup> transport in higher plants. *Annu. Rev. Plant Biol.* 54: 575-603.  
Google Scholar: [Author Only](#) [Title Only](#) [Author and Title](#)
- Véry, A.-A., Nieves-Cordones, M., Daly, M., Khan, I., Fizames, C., and Sentenac, H. (2014). Molecular biology of K<sup>+</sup> transport across the plant cell membrane: what do we learn from comparison between plant species? *J. Plant Physiol.* 171: 748-769.  
Google Scholar: [Author Only](#) [Title Only](#) [Author and Title](#)
- Wang, R.S., Pandey, S., Li, S., Gookin, T.E., Zhao, Z., Albert, R., and Assmann, S.M. (2011). Common and unique elements of the ABA-regulated transcriptome of *Arabidopsis* guard cells. *BMC Genomics* 12: 216.  
Google Scholar: [Author Only](#) [Title Only](#) [Author and Title](#)
- Wang, X.P., Chen, L.M., Liu, W.X., Shen, L.K., Wang, F.L., Zhou, Y., Zhang, Z., Wu, W.H., and Wang, Y. (2016). AtKC1 and CIPK23 Synergistically Modulate AKT1-Mediated Low-Potassium Stress Responses in *Arabidopsis*. *Plant Physiol.* 170: 2264-2277.  
Google Scholar: [Author Only](#) [Title Only](#) [Author and Title](#)
- Wegner, L.H., Boer, A.H. De, and Raschke, K. (1994). Properties of the K<sup>+</sup> inward rectifier in the plasma membrane of xylem parenchyma cells from barley roots: effects of TEA<sup>+</sup>, Ca<sup>2+</sup>, Ba<sup>2+</sup> and La<sup>3+</sup>. *J. Membr. Biol.* 142: 363–379.  
Google Scholar: [Author Only](#) [Title Only](#) [Author and Title](#)
- Wille, A.C., and Lucas, W.J. (1984). Ultrastructural and histochemical studies on guard cells. *Planta* 160: 129-142.  
Google Scholar: [Author Only](#) [Title Only](#) [Author and Title](#)
- Zhang, B., Karnik, R., Wang, Y., Wallmeroth, N., Blatt, M.R., and Grefen, C. (2015). The *Arabidopsis* R-SNARE VAMP721 interacts with KAT1 and KC1 K<sup>+</sup> channels to moderate K<sup>+</sup> current at the plasma membrane. *Plant Cell* 27: 1697-1717.  
Google Scholar: [Author Only](#) [Title Only](#) [Author and Title](#)
- Zhao, Z., Zhang, W., Stanley, B.A., and Assmann, S.M. (2008). Functional proteomics of *Arabidopsis thaliana* guard cells uncovers new stomatal signaling pathways. *Plant Cell* 20: 3210-3226.  
Google Scholar: [Author Only](#) [Title Only](#) [Author and Title](#)
- Zhou, L.H., Liu, S.B., Wang, P.F., Lu, T.J., Xu, F., Genin, G.M., and Pickard, B.G. (2017). The *Arabidopsis* trichome is an active mechanosensory switch. *Plant Cell Environ.* 40: 611-621.  
Google Scholar: [Author Only](#) [Title Only](#) [Author and Title](#)
- Zhu, M., and Assmann, S.M. (2017). Metabolic signatures in response to abscisic acid (ABA) treatment in *Brassica napus* Guard cells revealed by metabolomics. *Sci. Rep.* 7: 12875  
Google Scholar: [Author Only](#) [Title Only](#) [Author and Title](#)